EIC Yellow Report

November 16, 2020

Editor:
LALAL

Contributors:
X. XYZ[1],

[1]Brookhaven National Laboratory, USA

Contents

Part I

Executive Summary

Chapter 1

The Electron-Ion Collider

Chapter 2

Physics Measurements and Requirements

Chapter 3

Detector Concepts

Chapter 4

Opportunities for Detector Technology and Computing

Part II

Physics

Chapter 5

Introduction

Chapter 6

The EIC Physics Case

Chapter 7

The EIC Measurements and Studies

Chapter 8

Detector Requirements

8.1 Inclusive Measurements

8.2 Semi-Inclusive Measurements

8.3 Jets and Heavy Quarks

8.4 Exclusive Measurements

8.5 Diffractive Measurements and Tagging

8.6 Summary of Requirements

Part III

Detectors

Chapter 9

Introduction

Chapter 10

Detector Challenges and Performance Requirements

10.1 Beam Energies, Polarization, Versatility, Luminosities

10.2 Rate and Multiplicities

10.3 Integrated Detector and Interaction Region

10.4 Backgrounds

10.5 Systematics and Ancillary Detectors

10.5.1 Luminosity

10.5.2 Polarimetry

10.6 Physics Requirements

Chapter 11

Detector Aspects

11.1 Magnet

11.2 Tracking

11.3 Particle Identification

11.4 Electromagnetic Calorimetry

11.5 Hadronic Calorimetry

11.6 Far-Forward Detectors

11.7 Electronics

11.8 Data Acquisition

11.9 Software, Data Analysis and Data Preservation

Chapter 12

The Case for Two Detectors

Chapter 13

Integrated EIC Detector Concepts

13.1 General Purpose Detector Concept

13.1.1 Standard Layout

13.1.2 Detector technology description

13.1.3 Electronics, Data Acquisition and Computing technology description

13.1.4 Detector Integration

Central Detector

Forward and Backward Detector

13.1.5 Systematics Discussion

13.2 Second General Purpose Detector Concept

13.2.1 Standard Layout

13.2.2 Detector technology description

13.2.3 Electronics, Data Acquisition and Computing technology description

13.2.4 Detector Integration

Central Detector

Forward and Backward Detector

13.2.5 Systematics Discussion

Chapter 14

Detector Technology

In this report, the EIC community motivates the need for two general-purpose detectors. With this in mind, different specific detector concepts with complementary designs have been developed, studied, and are described in previous chapters. While significant progress has been reached in developing these concepts, work is still needed to ensure that the respective detector technologies reach a viable state of maturity for construction readiness and EIC science.

The need for R&D was realized early by the community and laboratories and in January 2011 Brookhaven National Laboratory, in association with Jefferson Lab and the DOE Office of Nuclear Physics, created a generic detector R&D program to address the scientific requirements for measurements at an EIC. The primary goals of this program were to develop detector concepts and technologies that have particular importance to experiments in an EIC environment, and to help ensure that the techniques and resources for implementing these technologies are well established within the EIC user community. It was also meant to stimulate the formation of user groups and collaborations that will be essential for the ultimate design effort and construction of the EIC experiments.

This program is, at the time of writing of this report, supported through R&D funds provided to BNL by the DOE Office of Nuclear Physics and is open nationally and internationally to the whole EIC community. Funded proposals are selected on the basis of peer review by a standing EIC Detector Advisory Committee consisting of internationally recognized experts in detector technology and collider physics. This committee meets approximately twice per year, to hear and evaluate new proposals, and to monitor progress of ongoing projects[1]. The program is administered by the BNL Physics Department.

Many of the supported projects, ongoing or completed, developed technologies that are now integral parts of existing detector concepts or are regarded as potential alternatives. The vertex detector R&D consortium, eRD25, aims to develop new improved MAPS sensors to meet the requirements demanded by the EIC requirements. Various MPGD tech-

[1]The web site of the generic R&D program with a description of the projects and all related documents and presentations is `https://wiki.bnl.gov/conferences/index.php/EIC_R%25D`.

nologies, such as GEM, Micromega, and µRWELL, have been pursued by the tracking consortium, eRD6, for low material tracking in barrel and forward regions as well as TPC readouts. New concepts like miniTPCs and integrated Cherenkov-TPCs had been developed and tested. Many options for electromagnetic, and recently, hadronic calorimetry have received R&D effort. From this grew the W-SciFi calorimeter, scintillating fibers embedded in a W-powder composite absorber. In parallel, novel scintillating glasses have been developed with unprecedented quality as an alternative to expensive $PbWO_4$ crystals. The particle ID consortium, eRD14, is pursuing various technologies, such as DIRC, dual RICH with gas *and* aerogel radiators, and new coating materials like nano-diamonds to replace CsI for RICH photo sensors are under investigation in eRD1. Time-of-Flight detectors, as well as Roman Pots for forward proton detection, require highly segmented AC-LGAD sensors whose development has just started to get supported by the program.

Besides hardware R&D the program supports various vital projects such as machine background studies and simulation software developments to enable more accurate definition of the physics' requirements. Sartre and Beagle are two examples of Monte-Carlo event generators whose development was substantially boosted by the program. Both were intensively used in the context of this report.

The generic R&D program was and is a vital part of the overall EIC efforts with over 280 participants from 75 institutions. Despite moderate funding, many groups are making excellent progress on many vital technologies needed for an EIC detector. The generic R&D program was not the only source of support for R&D relevant for an EIC detector. Several National Laboratories, among them BNL, JLab, ANL, and LANL, supported EIC detector R&D through Laboratory Directed Research & Development Programs (LDRDs) and many university groups in and outside of the US, active in the many R&D projects received support from their respective department and/or funding agencies. The EIC also benefited substantially from R&D conducted for many HEP and NP experiments such as ALICE and LHCb at CERN, Panda at GSI and Belle-II at KEK.

In the coming years the generic R&D program will be replaced by a targeted program funded out of the EIC project and guided by a Detector Advisory Committee (DAC). However, the community sees also a need for a continuation of a more generic program to support technologies that go beyond the immediate needs of a day-1 detector.

In the following we discuss the remaining R&D needs for technologies that are candidates for being deployed in a multi-purpose EIC detector. Here we do not distinguish areas of targeted R&D, *i.e.*, R&D needed to ensure a functional baseline EIC detector on day-1 and more generic R&D, *i.e.*, more future-looking detector concepts and technologies that have the potential to enhance the scope of EIC science in the outyears. The respective timelines are indicated in the individual section.

14.1 Silicon-Vertex Tracking

14.1.1 Monolithic Active Pixel Sensors (MAPS)

The EIC requires precision tracking with very low X/X_0. The goal of MAPS R&D is to develop sensors that meet the stringent EIC requirements for vertexing and tracking. The combination of very high single point spatial resolution (< 5 μm) and very low mass detector layers makes MAPS technology the most suitable candidate. More specifically, work is underway at CERN on a 65 nm MAPS detector for the ALICE ITS3 project and it is suggested that joining this development is the most efficient route to an EIC MAPS detector. The advantage of this route is that the design parameters for the ITS3 based sensor technology closely match EIC needs, including 10 μm^2 pixels (very precise spatial resolution), low power dissipation (reduced needs for cooling and power delivery leading to reduced infrastructure) and sensors thinned to 30-40 μm (low X/X_0). Furthermore, there are significant advantages in joining a well-funded and staffed existing design effort (high likelihood of success). The ITS3 work is already underway, so funds and support would be needed rapidly to enable full exploitation of this opportunity. An additional consideration is that further effort and funds would be needed to adapt the existing ITS3 design goals to an EIC specific sensor for the barrel and disc layers. The needed R&D is to support the development of a MAPS sensor based on the ITS3 effort currently underway at CERN. The work done will follow the path of the eRD-25 effort and the EIC silicon consortium. The goal of this consortium is to develop a MAPS sensor and associated powering, support structures, control and ancillary parts as necessary to produce a detector solution for silicon tracking and vertexing for the central tracking parts of an EIC detector. This will include significant design, testing, prototyping and the groundwork/R&D to lead to a funded construction project. A more detailed description of the current path that leads to an EIC optimized sensor and associated infrastructure can be found in the eRD-25 proposal[2].

It is critical that this effort be supported immediately and continuously to allow for the integration of the EIC based design and testing team into the ITS3 effort and to allow for the contribution of the EIC consortium members to the developing design. Looking at the schedule for this development to lead to an EIC optimized sensor in the time-frame needed for detector construction, delay would seriously impact the likelihood of success. The product of this effort can be used at either or both interaction points. It is intended as a full silicon based inner tracking and vertexing solution. The overall designs (number of barrel layers and discs, spacing, etc.) may be different for each region, but the need for high precision inner tracking/vertexing is likely to be present at both detectors. The timeline is indicated in detail in the FY21 eRD-25 proposal. This effort is needed for a day-1 detector and would be very applicable to subsequent/parallel efforts for a detector at the second interaction point.

[2]See https://wiki.bnl.gov/conferences/images/6/6d/ERD25-Report-FY21Proposal-Jun20.pdf

14.1.2 Silicon-Sensor Tracking Fallback

The goal of sensor tracking fallback R&D is to monitor developments in 180 nm MAPS, Silicon on Insulator (SOI) and LGAD technologies that can be developed into tracking sensor solutions for EIC tracking. It is prudent to keep abreast of developing sensor technologies and to plan for a fallback solution should the 65nm MAPS development in collaboration with the ALICE ITS3 project prove to be unsuitable for this purpose.

The combination of very high single point spatial resolution (< 5 μm) and very low-mass detector layers leads to the selection of silicon based sensors for EIC tracking. While a path to meet the EIC requirements using 65 nm MAPS technology has been identified, production of sensors for construction of an EIC tracking detector should begin in the 2026 time-frame in order for a detector to be ready for use in the 2030 time-frame. During this development time, contingency plans using other technologies should be developed. The most promising existing technology for a fallback path is 180 nm MAPS based on ALPIDE or Depleted MAPS sensors such as MALTA. The pros are having an alternative path to success should the existing effort be unsuitable due to technology or schedule considerations. The cons are that general silicon R&D can be expensive in both material costs and effort and having two parallel path of MAPS development might be prohibitive. While this is not the primary path, this could become the primary path to having a sensor that meets the EIC requirements available in the needed timeframe.

The path involving the least amount of additional development is through the adaptation of existing 180 nm designs. At this point it is still prudent to maintain a close watch on the developing technologies of SOI and LGADs as progress is being made in both technologies. Doing the baseline R&D to develop a fallback path is urgent and increases the chances of having a sensor available that meets EIC requirements in the needed timeframe. This should be explored in the 180 nm technologies. This effort should be done in parallel with the timelines developed for the primary ALICE ITS3 based effort on 65 nm MAPS. This effort is needed for a day-1 detector and would be very applicable to subsequent/parallel efforts for a detector at the second interaction point.

The LGAD technology offers very high temporal resolution (tens of ps) and is also a candidate for TOF and bunch crossing timing at the EIC. Whilst MAPS technologies have proven low mass, low power dissipation and very high single point resolutions to match EIC vertex and tracking requirements, these features are not yet available in state-of-the-art LGAD sensors. R&D in this direction is however undertaken by a number of HEP groups and progress should be monitored.

14.1.3 Services Reduction – Multiplexing and Serial-Fiber Off Detector Output

The primary goal for this R&D is to reduce services loads by reducing the number and volume of the way that data is taken off of the silicon tracking and vertexing detector. This effort will need to balance the reduction in service loads with the risks of losing communication with larger parts of the detector in the event of single point failures. It is possible

that even with redundancy, one would be able to reduce the service loads significantly. While this is primarily geared for the silicon tracking barrel layers and discs, the product of this R&D could apply to other detectors in the main detector volume. The product of this R&D would be envisioned for a day-one EIC detector, but also could be improved for future detector upgrades.

The envisioned EIC requirement is the need for the reduction of the services loads and corresponding space and radiation length reduction. This matches the need for very low radiation length of non-active parts of the detector. Most of these services will exist in the acceptance of the parts of the tracking detectors and most of the acceptance of the surrounding detectors (PID, Calorimetry, etc.) The advantages are what has been described. The risks could be related to single point failures and the hope that redundant paths with higher bandwidth and lower mass connections could ameliorate this yielding net positive results.

R&D would be needed in radiation tolerant multiplexing (probably using radiation tolerant FPGAs) and in high speed (5 GHz and above) fiber or multi-fiber optical transmission components. Both of these technologies are complimentary and urgent. This R&D, while initially envisioned for the silicon tracking/vertexing detector, can be applied to other detector readout systems. In general, the application of this type of R&D benefits most when it is co-developed with the detector technology (MAPS sensors, GEMS, etc.). This research could also compliment and integrate additional efforts in moving some of the early stage analysis onto the detector (providing track candidates, etc.). This R&D could lag the primary sensor R&D by up to 6 months as an estimate, but should be considered as part of the system level approach to developing detector solutions. This is envisioned for a day one detector implementation.

14.1.4 Services Reduction - Serial Powering and/or DC-DC Converters for Powering of Detector Components

This R&D aims at reducing the services loads by minimizing the number and volume of the primary service load of the silicon tracking and vertexing detector, the power and return cables. The magnitude of this load in existing architectures has been documented in detail (see section 11.2.11). This effort envisions investigating both possibilities of serial powering, possibly with on chip regulation and the use of on detector radiation tolerant DC-DC converters, either or both of which could significantly reduce the required amount of power cabling. While this is primarily geared for the silicon barrel tracking layers and discs, the product of this R&D could apply to other detectors in the main detector volume. The product of this R&D would be envisioned for a day-one EIC detector, but also could be improved for future detector upgrades. The envisioned EIC requirement is the need for the reduction of the services loads and corresponding space and radiation length reduction. This matches the need for very low radiation length of non-active parts of the detector. Most of these services will exist in the acceptance of the parts of the tracking detectors and most of the acceptance of the surrounding detectors (PID, Calorimetry, etc.) The advantages are what has been described. The risk could be related to single point fail-

ures in the serial powering chains which, depending on the architecture, could cause loss of powering to larger segments of the detector, and limitation in the current scaling factor for integrated DC-DC converters. The architectural aspects would be a significant part of the R&D.

This effort envisions investigating both possibilities of serial powering, possibly with on chip regulation and the use of on detector radiation tolerant DC-DC converters. Both of these technologies are complimentary and urgent. This R&D, while initially envisioned for the silicon tracking detector, can be applied to other detector powering systems with commensurate improvements in the powering services loads. In general, the application of this type of R&D benefits most when it is co-developed with the detector technology (MAPS sensors, GEMS, etc.). This R&D could lag the primary sensor R&D by up to 6 months as an estimate, but should be considered as part of the system level approach to developing detector solutions. This is envisioned for a day one detector implementation.

14.1.5 Fast Timing Silicon Technologies

COMMENT-TU: Merge with 14.1.2.

The proposed silicon vertex/tracking detector will be built around the beam pipe and is close to the beam interaction region of the EIC. High beam background such as synchrotron radiation generated by keV electrons and MeV neutron gas could generate dead areas in the silicon detector which significantly impacts on its vertex/tracking capability. To achieve precise measurements in Semi-Inclusive Deeply Inelastic Scattering (SIDIS) processes, event separation from different collisions is required. A radiation hard and fast timing silicon detector, which can survive the accidental beam injection onto the detector and is capable to separate the 1-10ns EIC bunch crossings, will enhance the physics measurement precision and could reduce the correlated systematical uncertainties.

To meet these requirements, various Si technology options have been considered, which are 1) High-Voltage or Depleted Monolithic Active Pixel Sensor (HV-MAPS or DMAPS) and 2) the Low Gain Avalanche Detector (LGAD). The HV-MAPS technology process fully depleted charged particle propagation inside the active silicon region. This technology can reach relatively low material budgets ($< 0.5\%\ X_0$ per layer), fine spatial resolution ($<$ 10 μm) and fast timing ($<$ 5 ns). The ongoing R&D will further improve the performance for the next-generation sensor production. Meanwhile, we also consider the LGAD [1–4] or AC-LGAD [5] technology to be placed in the most forward planes in the hadron-endcap region, which can provide fast time stamping to separate different bunch crossings. The HV-MAPS (or DMPAS) technology such as MALTA [6–8], ATLASPIX3 [9] or Mupix [9] could be implemented for the EIC day-1 detector. The LGAD or AC-LGAD technology could be used for EIC detector upgrade depends its R&D progresses. The performance of the LGAD (AC-LGAD) and MALTA technology has been summarized in Table 14.1.

The advantages of the MALTA technology are: 1) prototype sensor and front-end readout electronics exist; 2) its spatial and temporal resolutions have been demonstrated by previous/ongoing bench/beam tests; 3) this technology with further developments with the

Parameter	LGAD or AC-LGAD	MALTA
Technique	Low Gain Avalanche Diode	180 nm Tower Jazz HV-MAPS
Pixel size	current 1.3mm $\times$ 1.3mm towards 100 μm $\times$ 100 μm, $\sim$10 μm spatial resolution is achieved with the new design.	36.4 μm $\times$ 36.4 μm, $\sim$ 7 μm spatial resolution.
Integration time	300-500 ps	$<$ 5 ns
Thickness per layer	$< 1\% X_0$	$< 0.5\% X_0$
Power consumption	under R&D	80 mW/cm^2
Noise level	under R&D	10^{-5} with low threshold
Radiation tolerance	$\sim 1.5 \times 10^{15}$ n$_{eq}$/cm^2	$> 10^{15}$ n$_{eq}$/cm^2

Table 14.1: Comparison of the LGAD and MALTA sensor performance

TowerJazz new production line could be available and in production stage within around 2 to 3 year time scale. The power consumption of the MALTA sensor is relatively higher than the existing ALPIDE sensor. Although it is in a reasonable scale, additional R&D for the next generation sensor developments and dedicated mechanical structure design are needed. The advantages of the LGAD technology are: (1) prototype sensor and front-end readout electronics exist; (2) fast timing ($\sim$20ps) provided by the LGAD technology can not only be used for time stamping but also for PID purpose. This technology is in early R&D stage, and the full readout chain needs to be defined.

The required R&D path includes back-end electronics and the readout full chain integrations. The most critical (urgent) item is ASIC design and readout developments. The HV-MAPS or DMAPS technology (e.g. MALTA) could use the same production line at the TowerJazz company as the ITS-3 technology. We could share the R&D on sensor developments, readout integration and the EIC silicon/vertex detector conceptual design. The approximated timeline for the relevant R&D is: Ongoing detector R&D work which includes the silicon sensor characterization and down selection from 2020 to 2022. Continued R&D efforts which focus on the readout chain developments for the EIC day-1 detector from 2022 to 2025 depends on the funding availability.

14.2 Tracking

14.2.1 Low-Mass Forward/Backward GEM Detectors

Gas Electron Multipliers (GEMs) are a well-established MPGD detector technology that will soon be operational on a large scale in current NP and HEP experiments, *e.g.*, SBS tracker, ALICE TPC upgrade, and CMS muon upgrade. In a day-one EIC detector, they can provide cost-efficient fast tracking with good spatial resolution in the forward and backward regions because they can cover a large area. For the same reason, GEMs could also be employed as muon detectors at the outside of the detector.

The requirements on the momentum resolution are summarized in Sec. **??**. Early simulations using EICroot for 10 GeV pions showed that for a detector geometry with vertex tracker, TPC, six forward MAPS disks, and with three GEM detector layers each placed in front and behind a RICH vessel, the momentum resolution with a 1.5 T magnetic field is $\sigma_p/p \leq 1.5\%$ in the GEM acceptance region $1.2 < \eta < 1.7$, which is close to meeting the backwards requirements. In the GEM acceptance region $1.7 < \eta < 3.1$, the resolution is above 1.5% rising to about 3% at $\eta = 3.1$. Unlike the requirements, it was observed in the simulation that the resolution does not grow exactly linearly with momentum at higher momenta. For example, for a 40 GeV pion at $\eta = 2.0$, the resolution is $\sigma_p/p = 4\%$, which meets the backwards requirement.

The available material budget is 5% of X_0. In the active area of one foil-based Triple-GEM detector layer, the material accounts for 0.6% of X_0. Consequently, up to eight layers could be installed in an EIC detector, e.g. four in front of a RICH and four behind it.

To bring low-mass GEM tracker technology to a state where it can be implemented in an EIC detector some R&D is still required: Improvements in the simulations and a second beam test.

The simulations need to be repeated and refined in the new fun4all simulation framework. Actually measured spatial resolutions and realistic support materials need to be incorporated properly into the simulation, in particular the materials in the TPC endplates, MAPS support structures, and the GEM support frames. Their impacts on forward/backward tracking performance and RICH seeding need to be fully quantified. This should take six months to a year to complete.

For the glued UVa prototype built at UVa different types of zebra strip connectorizations need to be tested. The mechanically-stretched FIT prototype with carbon fiber frames has been undergoing major refurbishments of it mechanics and its operation needs to be confirmed. If successful, both prototypes will be evaluated in a second beam test at Fermilab planned for Spring 2021 to finalize the spatial resolution studies and the overall performance characterisation of the prototypes.

14.2.2 Large Cylindrical μRWELL Layer

One significant need for large cylindrical μRWELL layers in the central barrel region is to provide high angular resolution for barrel PID detectors. This additional tracking information can aid in the PID particle seed reconstruction, leading to better particle separation. For the scenario where a TPC is chosen as the central tracker option for the EIC detector and MAPS technology is adopted for the vertex tracker, we have identified two additional motivations for the need of a high-precision and fast-signal tracking detector to complement the inherent limitations of the TPC + MAPS as main tracking detectors in the barrel region. The first is to have the cylindrical μRWELL layer serve as a high space point resolution tracking layer to aid in the TPC field distortion corrections and TPC calibrations. The second need would have the cylindrical μRWELL serve as a fast (a few ns) tracking layer to compliment the relatively slow TPC and MAPS detector suite.

The simple construction of a μRWELL detector relative to a triple-GEM detector makes it an ideal MPGD technology to use in a cylindrical geometry. However there are still several R&D items related to its construction and performance that still need to be investigated. The first is related to the μRWELL technology itself. Efforts are needed to reduce the overall material budget of the current "standard" μRWELL. This involves the development of low mass amplification and readout structures. Ideally the cylindrical μRWELL would consist of one large foil and thus have no dead region in the active area. However, like with GEMs, μRWELL raw material is limited to a width of about 50 cm. To provide proper coverage for a barrel PID detector, several μRWELLs will be needed to form the full cylindrical layer. R&D is needed to determine best way to integrate the μRWELLs into one large cylindrical detector while minimizing dead regions in the active area.

Another area of R&D that is needed is related to the support structure of the cylindrical μRWELL layer. This involves developing large, high strength and lightweight cylindrical μRWELL supports to hold the detector's cylindrical shape. Additionally, end cap structures to hold the cylindrical detector in place need to be designed.

Several performance studies such as rate capabilities, dE/dx, tracking, and timing resolutions need to be carried out with the detector operating in a μTPC mode. These results will help to determine the proper readout electronics that are needed. The detector's cylindrical uniformity, discharge rate and aging properties will also need to be assessed.

14.2.3 Large Micromegas Barrel Tracker

The central region of the EIC detector requires very low material budget sub-detectors. Large area Micro-Pattern Gaseous Detectors are a possible solution to complement the silicon vertex detector. In particular, Micromegas detectors have been already successfully employed for building compact and light trackers, such as the Barrel Micromegas Tracker (BMT) of the CLAS12 experiment at the Jefferson Lab. Studies conducted within the Yellow Report effort showed that a barrel tracker made of MPGD tiles of a similar technology to the CLAS12 BMT one, would fulfill the requirements in terms of material budget and tracking resolutions. The CLAS12 BMT consists of six concentric layers of curved resistive Micromegas detectors where each layer is composed of three tiles of about 120 degrees width. The material budget of on tile in the active area is about 0.3% of X_0. From the experience of the CLAS12 BMT, the R&D on the EIC tracker will have two main objectives: reducing even more the material budget and simplifying production and integration.

In the CLAS12 BMT, the thickness of the self-supporting curved detector is determine by the ability to maintain the desired curved shape when constrained at both end by the carbon structure. The material thickness is $\sim$ 200 μm FR4 for a radius of $\sim$400 mm. Reducing the thickness further requires R&D, initially of flat stretched detectors using Micromegas made on a Kapton film of 50 μm. A detector will consists of two stretched foils (readout and drift) on a carbon frame with pillars to maintain and control the drift distance. Two additional external thin foils (made of 10 μm polypropylene) will hold the gas pressure instead of the thin electrodes. The R&D should start with the choice of optimal material

followed by a full size prototype to demonstrate the integration technique.

Curved detectors impose the use of specific sizes and tools for each curvature radius, thus making the production line more complicate. Excessive large area detector elements require numerous tooling to handle and to control the mechanical uniformity. A modular flat detector that would allow a higher production yield rate and possibly reduce the costs. The necessary R&D will need study a thin support structure to integrate this modular design.

On most MPGDs, copper is the chosen readout material with a thickness of at least 9 μm. The use of lower mass material for the strip readout such as metalized aluminum of about 0.4 μm requires R&D. The aluminum strips will have to be protected by a resistive layer to prevent vaporization of the metalized layer due to sparks.

The standard thinnest mesh used for large surface Micromegas detectors is a stainless-steel woven mesh of 18 μm wires. The alternative solution is electro-formed meshes (i.e Nickel of 10 μm) which are expensive, very fragile and limited in size ($\sim$ 30 $\times$ 30cm^2). Since 2018, in parallel with the use of laser techniques for etching "zigzag" patterns, a proof of concept has been made of laser etching holes on a small surface with different material (Cu, Al, Steel) of varying thicknesses (10, 15, 20 μm). R&D is needed to study this technique on larger surfaces to obtain large thin stretched aluminum foil with millions of holes to be used in the Micromegas bulk process.

Standard connectors made of plastic and brass contacts are quite heavy in term of material budget. If the active area is segmented, the multiplication of connectors can be a problem. Further R&D will test kapton-kapton connections with metal pixels clamped with light materials (carbon or 3D printed plastic).

14.2.4 R&D Needs for Planar μRWELL Detectors

COMMENT-TU: Are all the (nested) subsection needed? It's a 1 page article. Please avoid to structure the article in bullets.

μRWELL is a promising MPGD alternative to the well established GEM or Micromegas detectors for tracking in EIC end cap regions. One significant advantage of μRWELL is that it combines its electron amplification stage (μRWELL foil) and the readout plane into a single device, making its fabrication simpler and more cost effective than GEM and Micromegas, specially for large area trackers. In addition, μRWELL are expected to be easier to operate and more stable under harsh radiation environment. These features makes large planar μRWELL an ideal option for EIC end cap trackers or as additional tracking layers in the Silicon - Gaseous hybrid configuration. μRWELL technology is also to be considered as amplification & readout layer option for TPC end cap readout or for transition radiation detectors (TRDs) required for electron identification.

R&D Needs for Large μRWELL Detector

As a relatively new MPGD technology, μRWELL have not been fully operated in an NP or HEP large scale experiment so far. Therefore, several area of R&D studies both generic and specific to EIC environment are still needed to fully validate this technology. Below is a list of a few identified R&D studies needed for EIC.

Generic R&D: Performances and stabilities of μRWELL technology

- **Rate capabilities and spatial resolution studies:** The impact of the uniformity of μRWELL resistive layer (DLC), for large area detector on the rate capabilities and spatial resolution performances required detailed R&D studies. Rate limitation is not expected to be an issue with μRWELL in EIC environment because μRWELL can operate at a rate of 100 kHz / cm^2, exceeding by a few order of magnitude the expected rate in the EIC end cap regions. However, these rate and spatial resolution studies performed on small prototypes require validation in beam test for large area detectors.
- **Discharge and aging properties of μRWELL:** With the introduction of the resistive (DLC layer) as one of the key component of μRWELL, several studies have demonstrated that μRWELL is, if not spark-free, a robust spark-resistant detector. Several studies also demonstrated the technology robustness against ageing in harsh particle environment. Additional R&D is required to study the best gas mixture for operation of the detector in a wide range of gain for applications at the EIC.

EIC specific R&D: Low-mass & large μRWELL trackers

In addition to the generic R&D on μRWELL technology, high performance tracking with radiation length in the EIC end cap region required dedicated R&D studies and prototyping for μRWELL . The required R&D, listed below, have strong synergy with the ones described in section 14.2.2.

- **Development of low-mass & large area μRWELL:** R&D efforts are needed to minimize the material budget of the current standard μRWELL to keep the radiation length around 0.4% per tracking layers. This means the development of a rigid PCB free detector and lightweight and narrow support structure based on high strength-to-weight ratio materials such as carbon fibers rather than standard G10 fiberglass frames.
- **Development of low mass 2D readout plane:** Another important R&D area is the development of high resolution low mass and low channel count flexible 2D readout layers to be coupled with the μRWELL amplification layer. A few new ideas for such readout planes are already being investigated

14.2.5 MPGD Readout for a Time Projection Chamber

In general, the TPC for the sPHENIX experiment can serve as a central tracking device in a Day-1 EIC detector. It has to undergo several upgrades and/or modifications in order to be optimized for the EIC program.
The sPHENIX TPC has been optimized to have a good momentum resolution which requires a good space point resolution for the tracks to be measured. The sPHENIX program does not require PID (dE/dx) to be performed with the TPC. Hence, the optimization for the sPHENIX TPC has concentrated on very good IBF suppression which sacrifices good dE/dx resolution. For the EIC program this feature has to be restored. In the EIC era it is also expected that IBF will not have the same significant impact as during the RHIC program.
For the introduction of a "new" TPC R&D consideration will be in the readout electronics section.

GEM and MicroMegas

Prospects for R&D are in the restoration of good dE/dx resolution. This requires the investigation on GEM-properties and different gas choices which find the optimum of relatively good IBF suppression and optimum dE/dx resolution.
The MicroMegas technology has the best intrinsic IBF suppression and is a good candidate for good dE/dx resolution. However, stability issues have to be investigated and is an indicator for R&D in the next time for pursuing the MicroMegas option.

Hybrid and Gating

A very promising candidate for combining very good IBF suppression and good energy resolution is the hybrid option of combining MicroMegas and GEMs into a single amplification stage. The MicroMegas acts as the main amplification stage and reduces the IBF to a minimum. The GEMs act as pre-amplifiers and provide the necessary field ratios to further suppress IBF. The combination of both technologies provide the robustness needed to operate in a high rate environment. First R&D projects have been already established and this amplification structure needs continued detailed investigation.
Gating grids that have been used in TPCs based on MWPC cannot be used in an EIC environment. The readout rate would not allow to cope with the luminosity requirement of the physics program. The requirement is that the TPC will be read out continuously which does not allow a traditional gating grid. Consequently, one has to investigate amplification devices that minimize IBF as described in the previous sections. R&D topics materialize in investigating gating device that work dead-time less. One of the option is to use a passive gating grid which "naturally" allows electrons to pass through the structure whereas ions will be attracted to a high degree and eliminated from the gas volume. The investigation of such structures has started and is ongoing.

Readout Electronics

An issue present for a TPC in an EIC environment is the material budget in the forward region, in particular the electron direction. One can possibly overcome this problem by introducing alternative readout electronics which presents at this time the major contribution to the material budget, including all its required infrastructure.
Possible candidates for improved readout electronics is the TimePix or similar constructed microscopic readout structured front-end electronics. The options are a (a) small sized TPC with microscopically sized readout pads, $\mathcal{O}(10^{-3}\,mm^2)$ and (b) a regular sized TPC with small sized readout pads, $\mathcal{O}(0.1\,mm^2)$.
Option (a) provides the registration of single electrons from the ionization trail of a track, acting as a form of digital camera. This would allow precise tracking and excellent dE/dx resolution. The R&D needs on this option are manifold, in particular gas choices and readout capabilities.
Option (b) would provide the registration of single clusters from the ionization trail of a track. This would allow precise tracking and excellent dE/dx resolution. The R&D needs for this option are in particular toward the adaptation of the microscopic readout structure of the front-end electronics and distribution over larger areas.
A further option for decreasing the material budget in the electron going direction of a TPC would be to investigate a single sided readout structure, i.e, having one readout plane whereas the other cap of the TPC consists of a thin cathode. This option would require feasibility studies.
All the above mentioned R&D topics should be investigated to a mature level until the final design of a possible central tracker in form of a TPC is established.

14.3 Particle Identification

14.3.1 A Modular RICH (mRICH) for Particle Identification

The mRICH is designed for providing PID capabilities for EIC experiments for kaon and pion separation in momentum coverage between 3 to 10 GeV/c and electron and pion separation around 2 GeV/c.

mRICH detector R&D has been supported within the EIC eRD14 Consortium since 2015. The key components of a mRICH module include a radiator (Aerogel, $\sim$10 cm $\times$ 10 cm $\times$ 3 cm, n = 0.03), a Fresnel lens (with focal length range from 3" to 6"), a mirror set, and a photosensor. The characteristic longitudinal dimension of a mRICH module is from 15 cm to 25 cm depending on the lens focal length. A realistic GEANT4-based simulation for mRICH has also been developed and verified with beam test data.

Two rounds of detector prototyping and beam tests were completed with a focus on verifying the detector working principle and performance. The results from the first beam test (in 2016) have been published in NIMA 871,2017. The second beam test was done in 2018 and the data analysis is still ongoing. Two more beam tests with particle tracking ca-

pability are under preparation in order to quantify the mRICH PID performance and new photosensors. One is planned at Fermilab in March of 2021 for testing the mRICH with a LAPPD. The groups involved in this test are BNL, ANL, SBU and GSU. The other test is planned at JLab Hall D in summer of 2021 using secondary electrons in momentum range from 1 to 6 GeV/c. The participating groups for this test include DukeU, INFN, JLab, USC and GSU.

Two key components of a mRICH module are the Aerogel block and a photosensor with single-photon detection capability and fine-segmented pixel size ($<$ 3 mm $\times$ 3 mm). The photosensor also needs to be working properly in high magnetic field.

To meet the needs of EIC experiments, a proper photosensor choice is critical. The planned beam test at Fermilab in March 2021 will help to evaluate the integration and performance with LAPPD. During the second mRICH beam test in 2018, three SiPM matrices were tested with varying cooling temperature range from -30 C degree to room temperature. This effort was led by Marco Contalbrigo at INFN, Ferrara. The radiation damage effects to SiPM performance is currently under study at INFN.

In regarding to the possible kinematic coverage in EIC experiments with mRICH modules, we recommend the following: **COMMENT-TU: Who is we? Recall the author is the EICUG. "recommend" sounds not right in the context of this section. Best would be to point on the needs of the mRICH earlier in the detector sessions.**

1. In electron endcap
2. In hadron endcap ($1 < \eta < 2.5$)
3. In central barrel region (assuming available space in radial direction $\sim$ 20 cm)

mRICH is considered as a day-1 detector given the EIC physics requirement for PID.

Besides the two planned mRICH beam tests in coming year, there is a longer-term R&D effort for mRICH toward engineering design which includes: (a) high quality mirror and mirror assembly; (b) mRICH holder box engineering for reducing total weight, easy assembling, and projective installation; and (c) continued test with available photosensor options.

14.3.2 A Dual-Radiator Ring Imaging Cherenkov Detector (dRICH)

The dual-radiator Ring Imaging Cherenkov (dRICH) detector is designed to provide continuous full hadron identification ($\pi/K/p$ separation better than 3σ apart) from $\sim$ 3 GeV/c to $\sim$ 60 GeV/c in the ion-side end cap of the EIC detector. It also offers a remarkable electron and positron identification (e/π separation) from few hundred MeV up to about 15 GeV/c. The baseline geometry covers polar angles from $\sim$ 5 up to $\sim$ 25 degree (pseudorapidity range $\sim 1.5 - 3$). Achieving such a momentum coverage in the forward ion-side

region is a key requirement for the EIC physics program. Currently, the dRICH is, by design, the only hadron identification detector in EIC able to provide continuous coverage in RICH mode over the full momentum range required for the forward end-cap.

The dRICH baseline configuration consists of six identical open sectors. Each sector has two radiators (aerogel with refractive index $n \approx 1.02$ and gas with $n \approx 1.008$) sharing the same outward focusing mirror and instrumented area made of highly segmented photosensors (3×3 mm^2 pixels). The photosensor tiles are arranged on a curved surface in a way that minimises aberrations. The original benchmark configuration assumed ~ 160 cm longitudinally long thickness but even a shorter, down to ~ 100 cm, dRICH preliminary version features a performance that fulfills the above mentioned key physics requirements, indicating a remarkable flexibility of possible dRICH configurations.

To meet the EIC specifications, critical elements are an effective interplay between the two radiators and a proper choice of the photosensor, that should preserve single-photon detection capability inside a strong magnetic field. The dRICH focusing system is designed to keep the detector outside the EIC spectrometer acceptance, in a volume with reduced requests in terms of material budget and radiation levels. This feature makes dRICH a natural candidate for the exploitation of magnetic field tolerant SiPMs with an integrated cooling system to mitigate their significant dark count.

The dRICH design and performance have been studied through various means: a full Geant4 simulation (including an event based particle reconstruction processor) [10], AI-based learning algorithms with Bayesian optimisation to maximise the hadron separation [11], analytic parameterisations taking into account the optical properties of each component and the Geant4 simulated resolutions.

A small-scale prototype is being developed to investigate critical aspects of the proposed dRICH detector, in particular related to the interplay and long-term performance of the two radiators and the simultaneous imaging. The prototype vessel is composed by standard vacuum parts to contain the cost and support pressures different from the atmospheric one. This would allow efficient gas exchange and, in principle, adjustment of the refractive index and consequent flexibility in the gas choice (in the search for alternatives to greenhouse gases). The prototype supports the usage of various type of photosensors, in particular SiPM matrices and MCP-PMTs.

A program has been initiated to study the potential of SiPM sensors for Cherenkov applications, aiming to an assessment of the use of irradiated SiPM in conjunction with the dRICH prototype. Promising SiPM candidates will be irradiated at various integrated doses (up to the reference value of 10^{11} n_{eq} cm^{-2}) and will undergo controlled annealing cycles at high temperature (up to 180 C). The SiPM response before and after irradiation will be characterised and their imaging potential will be studied with a customised electronics. High-frequency sampling and Time-of-Threshold-based readouts will be compared. Of particular interest, the ALCOR front-end chip designed to work down to cryogenics temperatures, features low-power TDCs that provide single-photon tagging with binning down to 50 ps and potential counting rate well exceeding 500 kHz per channel. The irradiated sensors will be cooled down to the working temperature (down to -40 Celsius) to instrument an

area suitable for imaging tests with the dRICH prototype. After an initial survey of the most promising candidates available on the market, a dedicated R&D could be pursued to meet the EIC specifications.

dRICH is considered as a day-1 detector given the EIC physics requirement for PID.

Besides the first SiPM irradiation campaign and the baseline prototype realisation in coming year, there is a longer-term R&D effort for dRICH toward engineering design which includes: (a) light and stiff support structure in composite materials (b) high quality mirror assembly; (c) cost-effective production of high-quality aerogel; (d) alternatives to the greenhouse gases; (e) magnetic field tolerant single-photon sensors; [10] (f) dedicated readout electronics and cooling.

14.3.3 Gaseous RICH with MCP-PMT

COMMENT-TU: It would be good to integrate that with the mRICH section above having one gaseous RICH section

The EIC TOPSiDE detector concept applies ultra-fast silicon sensors to achieve particle identification through time-of-flight measurements in the tracker and the electromagnetic calorimeter. Ring imaging Cherenkov (RICH) detector in the forward region is essential for high momentum hadron particle identification to complement the TOF-based approach. A forward gaseous RICH using Argonne 10×10 cm^2 MCP-PMTs is under development to cover forward angles up to 10 degrees for high momentum hadron identification.

Argonne MCP-PMT has demonstrated low dark count, high magnetic field tolerance and fine pixel readout as a promising photosensor candidate for EIC RICH detectors. For a gas RICH prototype construction, several larger format (10×10 cm^2) MCP-PMTs will be needed to cover the required area. Gas RICH prototype simulation and design optimization are undergoing to fit the TOPSiDE concept. A beamline test will be desired to validate detector prototype performance. The gaseous RICH with MCP-PMT effort is part of the TOPSiDE detector R&D, it aims at hadron particle identification of 10-50 GeV in TOPSiDE but can be shared with other Cherenkov detectors (GEM-gas RICH, dRICH, and mRICH), and applicable to other EIC detector concepts.

R&Ds need to be completed in two years, include the fabrication of Argonne $10\times$ 10 cm^2 MCP-PMTs, simulation and design of gaseous RICH prototype with MCP-PMTs for TOPSiDE, construction of gaseous RICH prototype, installation and test at Fermilab or JLab.

14.3.4 High-Performance DIRC

The high-performance DIRC (hpDIRC) is a proposed hadronic PID system for the barrel region of the central detector, capable of π/K separation with 3σ or more up to at least 6 GeV/c momentum over a wide angular range. It can also contribute to e/π identification at lower momenta and provide a supplemental time-of-flight measurement.

The hpDIRC is a compact system with a radial thickness of less than 8 cm. The design is flexible, the radius and length of the bars can be modified without impact on the PID performance and the shape of the expansion volume prism can be selected for optimum position of the sensors in the magnetic field. It has low demands on the detector infrastructure (no cryogenic cooling, no flammable gases) and is easy to operate. The R&D of the hpDIRC is at an advanced stage. The PID performance estimate is based on test beam results, with excellent agreement between simulation and prototype data.

Several areas still require significant R&D. Optimizing the cost efficient design, matched to the final EIC detector layout, in simulation and validating it with the full system hpDIRC prototype is the most critical item. Another example is developing a procedure to disassemble the BaBar DIRC bar boxes and extract high-quality radiator bars for hpDIRC. In addition, the hpDIRC requires "external" R&D by EIC groups working on developing the fast readout electronics for small-pixel MCP-PMTs and on pixelated LAPPD sensors. This R&D is important for several other EIC detectors as well. Significant funding is needed soon to upgrade the PANDA DIRC prototype, which is being transferred from GSI to CUA/SBU, to fully equip it with new sensors and electronics, in order to validate the resolution and PID performance with cosmic muons and/or particle beams. A new Cosmic Ray Telescope (CRT) facility is being developed for the hpDIRC in collaboration between SBU, ODU, and CUA to study the prototype prior to possible tests in particle beams. This CRT will be available for use by other EIC systems.

The feasibility of reusing the BaBar DIRC bars vs ordering new radiator bars, and of using LAPPDs instead of commercially available MCP-PMTs, have to be determined since they have a large impact on the projected cost. The recently discussed potential increase of the PID momentum coverage, required by EIC physics, may require additional design improvements and utilizing possible post-DIRC tracking. Since the discussions about higher magnetic field options for the EIC detector are still ongoing, further investigation of a sensor solution for a possible 3T field is required. If the funding for the continuation of the R&D program is made available, we expect the hpDIRC TDR readiness to be achievable by 2024/2025.

14.3.5 Photosensor: MCP-PMT and LAPPD

The choice of photosensors is essential for reaching the cost and performance goals of all EIC PID subsystems. The best possible photosensor solution for each detector component is driven by the detector's operational parameters, naturally with cost optimization in mind. Ultimately, it would be preferable to use a common photosensor thus reducing development and procurement costs.

Microchannel plate photomultipliers (MCP-PMTs) from commercial vendors have shown superior good timing and position resolution as well as high magnetic field tolerance but are generally far too expensive for large area coverage. The recently commercialized new type MCP-PMT using the atomic layer deposition technique as a large area picosecond photodetector (LAPPD) provides a promising cost-effective MCP-PMT for the EIC RICH

detectors. Efforts have already been devoted to optimizing the LAPPD as photosensor of choice for EIC Cherenkov detectors (e.g. dRICH, mRICH, DIRC) as well as TOF applications.

A list of performance requirements of the photosensors for EIC Cherenkov based detectors is listed in Tab. 14.2.

Parameter	gas-RICH, mRICH, dRICH	DIRC
Gain	$\sim 10^6$	$\sim 10^6$
Timing Resolution	$\leq$ 800 ps	$\leq$ 100 ps
Pixel Size	$\leq$ 3 mm	2–3 mm
Dark Noise	$\leq$ 5MHz/cm^2	$\leq$ 1kHz/cm^2
Radiation Hardness	Yes	Yes
Single-photon mode operation	Yes	Yes
Magnetic-field tolerance	Yes (1.5–3 T)	Yes (1.5–3 T)
Photon Detection Efficiency	$\geq$ 20%	$\geq$ 20%

Table 14.2: Performance requirements of photosensors for EIC Cherenkov based detectors.

R&D at Argonne National Laboratory using the Argonne MCP-PMT (6×6 cm^2), a small format of LAPPD, has demonstrated all the required parameters, especially a magnetic field tolerance over 1.5 Tesla and less than a 1 mm position resolution with a pixel size of 3×3 mm^2. To expedite the application of MCP-PMT for EIC Cherenkov detectors, a 10x10 cm^2 MCP-PMT fabrication facility is under construction to produce larger size, high-performance Argonne MCP-PMTs. The commercial LAPPD has also achieved almost all the requirements except fine pixel size and magnetic field tolerance. Our industrial partner has adapted the Argonne MCP-PMT R&D results to develop low-cost pixelated LAPPDs for EIC Cherenkov detectors. Fine pixel size (3x3 mm^2) is the urgent focus for commercial LAPPDs; bench and beamline tests are required for the LAPPD validation.

The Argonne MCP-PMT/LAPPD R&D is a generic effort. These photosensors can be widely used where large areas, low cost and high performance are needed. This R&D is aimed at both near-term and future detector designs. Testing and performance results have already been shared with all EIC Cherenkov and TOF detector design efforts.

Rapid progress has been achieved on the Argonne MCP-PMT/LAPPD. Recently, a Gen-II LAPPD was successfully tested at Jefferson Lab in a high rate, high background environment. Furthermore, a Fermilab beamline test of a pixelized MCP-PMT performance is planned for Spring 2021. To validate the LAPPD performance and apply this new technology to the EIC-PID subsystems, critical R%D is needed in the next two years. A bench test and multiple beam tests of Cherenkov prototype detectors using the MCP-PMT/LAPPD will need to be performed. For example, an mRICH beam test with LAPPD is mentioned in the mRICH section, and a gaseous RICH detector with Argonne 10x10 cm2 MCP-PMT is under development and planned for a beamline test as well.

14.3.6 R&D Needs for GEM-TRD/Tracker in the Forward Direction

Identification of secondary electrons plays a very important role for physics at the Electron-Ion Collider (EIC). A high granularity tracker combined with a transition radiation option for particle identification could provide additional information necessary for electron identification or hadron suppression. The scope of the project is to develop a transition radiation detector/tracker capable of providing additional pion rejection ($> 10 - 100$).

COMMENT-TU: would remove bullet and turn into plain prose. Matches better with rest.

- *TR Radiator:*
  Transition radiation radiator with low material budget available for a mass-production need to be identified, optimized and tested, for example, optimization of a pseudo-regular radiator using thin (12-15μm) kapton foils and thin net spacers, or a test of available fleece/foam materials for TR-yield.

- *Detector design:*
  The detector technology is inherited from GEM and considered as well established. The main difference is the thickness of the drift volume. To keep the electric field uniform in the large drift volume, a special field cage should be developed. Mechanical design and construction of the field-/gas- cage to minimize a Xe-filled gas gap between radiator and the drift cathode needs to be performed.

  The anode readout PCB layer of the current GEM-TRD prototype is based on the so-called COMPASS readout made of X and Y strips of pitch size of 400 μm, which is good for high occupancy environment, but the large number of channels increase the price for readout electronics.

  We have been working on a new concept of pad readout PCB as anode readout for MPGD technologies more suited to the GEM-TRD application. This novel large-pad readout PCB, by design, combines three crucial advantages that will greatly benefit GEM-TRD: large readout pad which means a small number of electronic channel to be readout, excellent spatial resolution despite the large pad size and we expect a better noise performance despite the the large size. Although zigzag readout option needs to be tested.

- *High voltage optimization:*
  GEMTRD needs 2 HV lines. One is for GEM amplification stage and another to set uniform drift field. To work in high occupancy environment, the drift time should be minimized, providing the field 2-3 kV/cm. for 2cm drift distance the HV should be at level of 4-5 kV. Depending on grounding scheme , the total voltage including GEM stage, could be up to 8-9 kV. Optimization of HV for large drift distances is ongoing.

- *Readout electronics:*
  GEMTRD currently use available readout from GlueX wire chambers. Preamplifier (GAS2 ASIC chip) with shaping time of 10-12ns. Flash ADC has sampling rate of 125MHz and 12 bit resolution. The total price is about $ 50 per channel. The collected

high resolution data at the test beam allow us to estimate the minimum needed shaping of preamplifier, FADC sampling rate and resolution. FADC125 board provides only pipe-lined triggered readout. A new development of FADC125 will be able to stream zero suppressed data over the fiber link is ongoing. Another possibility to adopt readout chip from other detectors, like SAMPA, etc..

- Gas system:
  Over the past few years, the price of Xe has gone up significantly. Design and Development of a recirculation system to purify, distribute, circulate, and recover the gas, based on a design of ATLAS TRD gas system at CERN.

14.3.7 Gaseous Single Photon Detectors Based on MPGD Technologies

Single Photon Detectors (PD) for Cherenkov imaging devices represent a key challenge at EIC where minimum material budget and operation in high magnetic field is required. Gaseous PDs, which have played /are playing a major role in establishing and operating Ring Imaging CHerenkov (RICH) counters, satisfy these requirements and they represent the most cost-effective solution when equipping large detector areas. So far, the only photon converter successfully coupled to gaseous detector is CsI with Quantum Efficiency (QE) limited to the far UV domain. Optimized detector architecture and operative conditions have to be established to ensure effective photoelectron extraction and control of the Ion BackFlow (IBF) to the photocathode. In particular, Micro Pattern Gaseous Detector (MPGD) technologies offer natural answers to IBF and photon feedback suppression and fast response, as tested by successful applications: the PHENIX HBD with triple GEM PDs [12], the COMPASS RICH upgrade with Hybrid (THGEMS and resistive MICROMEGAS) PDs [13], the windowless RICH prototype and test beam with quintuple GEM PDs [14], the TPC-Cherenkov (TPCC) tracker prototype with quadruple GEM PDs [15].

In the EIC context, gaseous PDs represent a valid option for the high momentum RICH with gaseous radiator. An R&D program for further developments of the hybrid approach in operation at COMPASS, aiming at making it fully adequate for the high momentum RICH at EIC, is ongoing, where the reduced space availability imposes a compact RICH. The whole program includes:

1. Establishing the hybrid PD for a windowless RICH approach to increase the number of detected Cherenkov photons;
2. Increasing the granularity of the read-out elements for fine resolution with limited lever arm; this item is well advanced;
3. Comparing the detector performance using either THGEM (as in COMPASS) or GEMs for the first multiplication stages;
4. Identification of an adequate front-end chip: studies for coupling the hybrid PD with VMM3 ASIC have been initiated;

5. Coupling of the THGEMs with a novel and more robust photoconverter by Hydrogenated Nano Diamond powder (HND) to overcome the limitation imposed by the use of CsI due to its chemical fragility in contaminated atmosphere or under ion bombardment, that imposes gain limitations and complex handing; very promising initial studies are ongoing.

The R&D will progress along these lines. The action items 1, 2, 3 and 4 are needed to make this technology adequate for its use at EIC and they can be completed within a couple of years. Establishing the novel photoconverter for gaseous PDs will take longer, due to the largely innovative character of the approach. If converging, it can represent an added value to the project. It can be selected for the EIC PDs according to its level of maturity when the detector design is finalized.

14.3.8 Fast Timing Silicon Sensor: LGADs

The Low Gain Avalanche Detector (LGAD) with internal gain [1, 16–20] is an ultra-fast silicon sensor technology, which has recently been chosen for constructing a fast-timing layer in the forward rapidity region of the CMS [21] and ATLAS [22] experiments at the high-luminosity (HL) LHC starting in 2027. The new timing layers will help the experiments mitigate significantly larger pileups of proton-proton interactions (up to about 200) by providing 4-D vertex reconstruction, and serve as a time-of-flight system for hadron identification in QCD and heavy-ion physics.

Traditional *n-p* silicon sensors with gains provided by external bias voltages can provide a typical time resolution on the order of 150 ps. The LGAD silicon sensors have an intrinsic gain of 10–30 provided by a special implant layer to generate a strong electric field locally and trigger avalanches. This internal gain helps the LGADs to achieve a low-jitter fast-rising pulse edge and overcome many other noise sources that enable high precision timing measurements for MIPs. LGAD sensors of 35–50 μm in active area thickness can achieve a typical time resolution of about 30 ps. The handling wafer has a tyical thickness of 150–300μm.

With excellent timing and position resolutions, the LGADs provide an attractive option for constructing a compact, multi-layer system to simultaneously provide TOF-PID and trajectory reconstruction as part of the tracking system. In addition, the LGADs have several other key advantages of being highly tolerant to strong magnetic fields (up to B$\sim$4 T), radiation-hard (up to $\sim 2 \times 10^{15}$ n_{eq}/cm^2, compared to the expected level of radiation of $\sim 10^{11}$ n_{eq}/cm^2 at EIC) and compact (flexible for integration). To fulfill the requirements for EIC physics, there are three main areas of R&D needed, which are discussed below:

- **Time resolution**: while LGAD silicon sensors used by CMS and ATLAS can provide a time resolution of 30–50 ps, particle flight distance at EIC detectors is likely to be much shorter due to tight space constraints. Therefore, a total time resolution (including readout electronics) of 20 ps or better per layer is desired to meet the PID requirement at low and intermediate momentum regions. The jitter contribution

to the time resolution is directly related to the signal slew rate, which is inversely proportional to the sensor thickness. Reducing the thickness from $50\mu m$ to 35, 25 and even $20\mu m$ will not only improve the jitter but can also suppress the Landau noise. Note that to maintain the total charge collection for a large signal, both internal and external gains applied also need to be optimized. Recent R&D work on $35\mu m$-thin LGADs shows a time resolution of about 20–25 ps per layer, a promising step toward achieving the PID requirements for EIC [23].

- **Fill factor and position resolution**: to serve as (part of) a tracking system, a position resolution much better than the 1 mm pixel size has to be accomplish to be competitive to other types of silicon pixel and/or strip sensors that are designated for position measurements. The current limitation lies in the approximately 50 μm width of the intra-pad no-gain region, which is needed to protect against early breakdowns. Smaller pixel sizes would lead to too low fill factors, or loss of acceptance. The CMS and ATLAS timing layers have a fill factor of 85% per disk, with the two-disk system compensating for a 100% acceptance.

  To achieve better position resolution (beyond 1 mm pixel size), two viable solutions are present. Trench-isolated (TI) LGADs is capable of reducing the no-gain region down to a width of only a few μm, essentially eliminating it to achieve 100% fill factor. All readout schemes can be kept the same as standard LGADs. For AC-coupled LGADs, segmentation is not done on the silicon sensor but at metallic readout contacts sitting on top of a dielectric layer, reading out induced charges. The fill factor is effectively 100%. The signal pulse is shared among several adjacent pads, further improving its position sensitivity. The metallic readout pads can be fabricated into pixels, strips or any shape desired. The AC-coupled LGADs are also considered as an option for a high precision timing Roman Pots, where R&D needs are discussed in Sec. 14.5.1.

- **ASIC readout chips**: The needs for better timing performance and finer granularity also pose significant challenges to the readout electronics and specifically to the ASIC readout chips. Present ASIC chips designed for CMS and ATLAS timing detectors have a jitter on the order of 20–30 ps, and a pixel granularity of 1.3×1.3 mm^2. Reduced granularity will make it more difficult to fit all the circuit components within the available space, and is also likely to lead to significantly increased power consumption due to increased total number of channels. Based on architectural designs of CMS and ATLAS timing layers, an ASIC chip with a size of 0.5×0.5 mm^2 is feasible to achieve and would meet the requirements set by the Roman Pot detector. A finer granularity, likely required for the tracker application, would require dedicated efforts of new architectural designs and adoption of more advanced silicon fabrication processes.

14.4 Electromagnetic and Hadronic Calorimetry

14.4.1 Tungsten Scintillator Calorimetry

Tungsten scintillator (W/Scint) calorimetry can play a major role in many of the regions of an EIC detector, covering a rapidity range from $\sim$ -2.0 to 4.0. It offers a very compact design in terms of its short radiation length, thus limiting the total length of the calorimeter, as well as providing a small ($\sim$ few cm) Moliere radius which limits the lateral extent of the shower, therefore allowing good separation between neighboring electromagnetic showers as well as limiting the overlap with hadronic showers. In addition, the energy resolution can be tuned by changing the sampling fraction and sampling frequency to meet the different requirements in the various rapidity regions.

There are primarily two candidates that are being considering for a W/Scint calorimeter for EIC. One is a tungsten scintillating fiber (W/SciFi) SPACAL, which consists of a matrix of tungsten powder and epoxy with embedded scintillating fibers. This technology is used for the sPHENIX barrel EMCAL that consists of more than 6K individual 2D projective absorber blocks. The blocks are read out using SiPMs that are coupled to the blocks using short light guides. This calorimeter is currently under construction and is expected to be completed by the end of 2021.

The technology for producing the blocks, which was originally developed at UCLA [24], has now been developed to produce these blocks on an industrial scale at the University of Illinois [25]. Therefore, no further R&D is required for producing the blocks. However, the method used for reading out the blocks with SiPMs could be improved. This would include the use of large area SiPMs to provide more photocathode coverage and eliminate the boundaries between the light guides which leads to non-uniformities in the energy response. It is planned to refurbish the sPHENIX EMCAL with this type of readout for use as a Day-1 detector at EIC.

The second W/Scint technology that is being considered for EIC is a tungsten shashlik (W/Shashlik) design. Many shashlik calorimeters have been built and used by many experiments. A W/Shashlik design offers some distinct advantages but also poses some significant challenges. In addition to being compact and being able to tune the energy resolution as in the W/SciFi, a W/Shashlik offers the possibility of improving the light collection and providing better uniformity by reading out each individual WLS fiber with its own SiPM. This allows a better determination of the shower position and the possibility of using this information to correct for non-uniformities in the energy response. However, the mechanical properties of tungsten make it difficult to machine and requires using a slightly less dense alloy of tungsten, thereby increasing the radiation length and Moliere radius. Also, making a shashlik calorimeter projective makes the mechanical design and assembly more complicated.

Both calorimeter technologies use SiPMs as photosensors, but it is well known that these devices are subject to radiation damage, particularly neutrons. The development of more radiation hard SiPMs would be of great benefit for calorimetry at EIC, as well as for many

other detectors, but developing radiation hard SiPMs would take several years of R&D and require a substantial investment with the manufacturers.

14.4.2 SciGlass for Electromagentic Calorimetry

Nearly all physics processes require the detection of the scattered electron in the electron endcap (forward rapidities). The requirement of high-precision detection is driven mainly by inclusive DIS where the scattered electron is critical for all processes to determine the event kinematics. Excellent electromagnetic calorimeter resolution of better than $2\%/\sqrt{E}$ is required at small scattering angles, while very good resolution is acceptable at larger angles. For hadron physics measurements with electromagnetic reactions, the most common precision calorimeter material of choice has been lead tungstate, $PbWO_4$ (PWO). However, the production of crystals is slow and expensive.

The technology goal of SciGlass R&D is to develop a scintillating glass for homogeneous electromagnetic calorimetry. SciGlass is a radiation hard material optimized to provide characteristics similar to or better than $PbWO_4$. SciGlass fabrication is expected to be cheaper, faster, and more flexible than $PbWO_4$ crystals. SciGlass is being developed by Scintilex, LLC in collaboration with the Vitreous State Laboratory at CUA. Tremendous progress has been made in the formulation and production of SciGlass that improves properties and solves the issue of macro defects. Scintilex has demonstrated a successful scaleup method and can now reliably produce glass samples of sizes up to $\sim$ 10 radiation lengths. Simulations combined with initial beam tests at photon energies of 4-5 GeV suggest that high resolution competitive with $PbWO_4$ can be reached for $> 15X_0$. SciGlass has excellent radiation resistance (no damage up to 1000 Gy electromagnetic and 1015 n/cm^2 hadron irradiation, the highest doses tested to date), response time of 20-50 ns, and good transmittance in the near UV domain (74% at 440 nm). The SciGlass insensitivity to temperature is also a clear advantage over $PbWO_4$, which has a dependence of about 2-3%/$^\circ$C and has to be continuously monitored. The present samples have a density up to 5.4 g/cm^3, radiation length (X_0) of 2.2-2.8 cm, and a Moliere radius of 2-3 cm.

The areas of needed R&D for SciGlass include the final formulation optimization, scale up to block sizes $\gtrsim 15X_0$, and beam tests to establish characteristics like energy resolution. The most critical items are to demonstrate scale up to block sizes $\gtrsim 15X_0$ and to establish SciGlass characteristics with beam tests. The evaluation of SciGlass as particle detector has been shared in part with activities on $PbWO_4$ crystals for the electron endcap calorimeter, *e.g.* simulations, radiator characterization and prototype construction, commissioning, and beam tests. The approximate timeline for completing the SciGlass R&D is about 1 year assuming R&D funds are available. The goal is to be ready for a day-1 detector. SciGlass could also be available for future detector upgrades.

14.4.3 Hadronic Calorimetry

Optimum jet reconstruction will require the use of several detector systems (tracking, EMCAL and HCAL) but is a main driver for hadronic calorimetry. As such, the requirements for the resolution of the hadronic calorimeter are different for the endcaps and the barrel region. The most challenging is the forward region of hadronic endcap where pure calorimetric measurements starts to outperform particle-flow like approaches due to the degradation of tracker performance. For the electron endcap and the barrel region, only modest hadronic energy resolution is required from calorimeter system (ECAL+HCAL). It is believed that these systems can be built using standard construction methods and no additional R&D efforts are needed. For the hadronic endcap, covering the rapidity range from $\sim$ 1.0 to 2.5 where better energy resolution is required, modest R&D efforts will be needed to improve the performance of these systems. For example, the STAR Forward Calorimeter, which is currently being constructed using a new and efficient method developed at UCLA [26, 27], would require improvements for a more efficient light collection scheme due to the relatively low energy of hadrons in this region of hadronic endcap at EIC.

At more forward rapidities in the hadron endcap, it is important to have the best possible performance of the calorimeter system. The main constrain at EIC is the lack of space for a high sampling fraction and high sampling frequency calorimetry system, both of which are required to achieve good resolution. Developing a high resolution calorimetry system for this region will require significant R&D efforts. At present we believe that there is only one technology option that may be suitable for this region, which is a very high density, approximately compensated fiber calorimeter, which would serve as both the EMCAL and HCAL with a common readout.

To date, R&D for hadron calorimetry for EIC has had a low priority and very limited funding. The synergy between the STAR Forward Upgrade and eRD1 R&D activities lead to construction and testing of two prototypes forward calorimeter systems. One was a compensated system with an EMCAL section built with a W/ScFi technique followed by hadronic section made of a lead scintillator sandwich. The other non-compensated version had a lead scintillating shashlyk EMCAL and an iron scintillator sandwich HCAL section behind. A later version was a final design prototype for STAR Forward Calorimetry system. Both versions had SiPM readouts and both were tested at FNAL. The performance of both systems led us to believe that the initial requirements for the EIC calorimetry system can be reached with only the modest improvements mentioned above. However, due to lack of funds, both versions of the prototypes had limited size which lead to significant transverse leakage and required an extrapolation of the test results to larger size detectors. This should be avoided for future EIC targeted R&D.

A common theme for the R&D needs for both an EMCAL and HCAL at EIC is the readout with SiPM sensors covering a large surface area. This may be challenging at the forward rapidities of the hadron endcap due to the relatively low light yield of hadron calorimeters (compared to EM calorimeters), and the high neutron fluences in this region, which will lead to significant degradations in SiPM performance. Operation of the STAR Forward

Calorimetry system in the 2022 500 GeV RHIC run will be very valuable because the conditions at STAR will be very close to those in the EIC hadron endcap in terms of neutron fluxes. Future R&D is therefore needed in this direction.

14.4.4 CSGlass for Hadronic Calorimetry

Achieving high-quality science at nuclear physics facilities requires the measurement of particle energy with excellent calorimeter energy resolution. Particles that produce EM showers can be detected with high precision. However, there is a need to improve the energy resolution of hadron calorimetry. The technology goal of CSGlass R&D is to develop a scintillating glass for improving hadronic calorimeter resolution, which is desired for measurements of hadronic jets.

CSGlass is optimized for the dual readout approach, where one compares the signals produced by Cherenkov and Scintillation light in the same detector. This approach has been a promising method to achieve better performance for hadron calorimeters. Homogeneous crystals are an option, but have to be outfitted with optical filters, which results in insufficient Cherenkov light detection. Crystals are also prone to radiation damage, time consuming to manufacture, and relatively expensive. In comparison, radiation-hard glasses can be tuned for favorable Cherenkov/Scintillation signal ratio, eliminating the need for optical filters, and thus offer great potential for both precision hadron calorimetry and significant cost reductions if competitive performance parameters can be achieved. CSGlass is derived from SciGlass and expected to be similarly resistant to EM and hadron irradiation up to 1000 Gy and 1015 n/cm^2, the highest doses tested so far. The CSGlass interaction length is comparable to crystals and should allow for small tower size. The anticipated space for the homogeneous calorimeter configuration could be similar to the binary system and may provide better resolution.

The areas of needed R&D for CSGlass include the demonstration of CSGlass with sufficient UV transparency for Cherenkov light collection, clear separation of Cherenkov and Scintillation light of sufficient intensity (slow scintillation, $>$ 500 nm beneficial), low cost, and characterization of CSGlass in the lab and with test beam R&D prototypes. The most critical items are the formulation optimization and production of CSGlass test samples. Some of the CSGlass R&D is shared with SciGlass and $PbWO_4$ crystals for EM calorimeters. The approximate timeline for completing the CSGlass R&D is $\sim$ 3 years assuming R&D funds are available. CSGlass could be ready for future detector upgrades.

14.5 Auxiliary Detectors

14.5.1 Roman Pots and LGAD Technology

A Far forward proton spectrometer, based on the well known technique of Roman Pots, is an integral part of an EIC detector system, essential for the success of its physics program

(see Secs. 8.4 and 8.5), and thus is envisioned as a subsystem for a day-one EIC detector. A forward proton spectrometer will provide a critical contribution to the study of inclusive diffractive and exclusive production processes in coherent e+p and e+D collisions. Furthermore, it is essential to provide a veto of incoherent background to measurements of exclusive meson production in e+A collisions, see Sec **??**. An innovative silicon technology, based on *Low Gain Avalanche Diode (LGAD)*, is proposed to instrument the Roman Pots, as well as other EIC detector subsystems, as it has the potential to combine in a single sensor fine spatial resolution and precise timing. More specifically, by AC-coupling the metal layer (that is connected to the readout electronics) to the active silicon layers of an LGAD (*AC-LGAD*), the sensor can be finely pixelated (in the order of few tens of microns) to reach a spatial resolution similar to conventional pixel trackers, and its timing performance can be maintained compatible to the one of standard LGADs, i.e. $\approx$ 30 ps. While the LGAD technology is established and is being used by the ATLAS and CMS experiments at the LHC for their timing subsystems for the High Luminosity phase (HL-LHC), the AC-LGAD technology is instead under intense development in US, Europe and Japan.

Simulations show that 500 μm square pixels and 30–40 ps time resolution are sufficient to achieve the desired physics performance. In more detail, simulations showed that the detector pixels must be at least as small as 500 x 500 μm^2 to make the smearing contribution negligible with respect to the other effects at 275 GeV. Currently available LGAD sensors for the HL-LHC have 1.3 x 1.3 mm^2 pixels, which would provide smearing contributions outside of the Roman Pots specifications. The 500 x 500 μm^2 pixelation can be achieved in AC-LGADs, and, with reasonable effort, in the associated readout electronics, i.e. by small modifications of the ASIC developed for the ATLAS timing detector. It must be noted that a space resolution an order of magnitude smaller than the pixel pitch can be achieved by using the information from the signal sharing between neighboring pixels, with a substantial advantage in power and real estate in the readout electronics. At the same time, in the high acceptance configuration, the impact of the angular divergence on the smearing of the transverse momentum becomes comparable to the contribution from the crab cavity rotation of the beam bunch. To remove the smearing contribution from the crab cavity rotation, in addition to further rejecting the backgrounds, fast timing is required in the range $\approx$ 30 – 40 ps. Such timing performance has been demonstrated by the LGAD sensors developed for the HL-LHC, and it has been recently shown to be achievable by AC-LGAD sensors too. In addition, such sensors must be placed as close as possible to the beam, therefore their inactive area at the edge of the sensor must be minimized, and must be $\leq$ 100 μm. Laboratory tests showed that the inactive edges of LGADs can be reduced to about 50 μm, i.e. to values compatible with the Roman Pots specifications.

In summary, the novel AC-LGAD sensor technology has recently been shown to meet both spatial and timing performance as well as small edge specifications for its application in Roman Pots. However, further work is needed to fully characterize the AC-LGAD performance, test their robustness and optimize their design for the specific implementation in Roman Pots. For instance, the intrinsic sensor gain and thickness can be optimized to improve the time resolution, finer spatial resolution can be achieved by exploiting the signal sharing properties of neighboring pixels, and larger area prototypes with advanced designs need to be fabricated and tested. Most critical at this point in time is the develop-

ment of an architecture of the readout electronics, and more urgently the ASIC R&D.

Given the need of fast-timing at EIC and the growing interests in LGAD technology to meet those needs (see time-of-flight detector, 4D tracker, TOPSiDE detector concept, 4π hybrid LGAD/SOI tracker, preshower), a collaborative effort will be extremely beneficial. An international consortium is being formed to accomplish the above-mentioned R&D tasks.

In a time-frame of 2 years, thanks to prototyping and laboratory testing, the AC-LGAD can be confirmed as the baseline technology for Roman Pots, while an optimization of the sensor readout can be achieved in a 5 year time scale. In a 2 year timeframe the readout architecture can be developed and its viability demonstrated via simulations as well as laboratory tests based on existing prototypes for the LHC, while in a 5 year time scale a more detailed design of the ASICs and the readout chain, including initial prototyping, can be achieved.

14.5.2 Zero Degree Calorimeter

The ZDC will serve critical roles for a number of important physics topics at EIC, such as distinguishing between coherent diffractive scattering in which the nucleus remains intact, and incoherent scattering in which the nucleus breaks up; measuring geometry of $e + A$ collisions, spectator tagging in $e + d/^3He$, asymmetries of leading baryons, and spectroscopy. These physics goals require that the ZDCs have high efficiency for neutrons and for low-energy photons, excellent energy, p_T and position resolutions, large acceptance and sufficient radiation hardness.

There are several possible approaches to achieve high energy and position resolution in a calorimeter. For example, the ALICE FoCal [28], is silicon-tungsten (Si+W) sampling calorimeter with longitudinal segmentation. Low granularity layers are used for the energy measurement while higher granularity layers provide accurate position information. A schematic of FoCal is shown in Fig. 14.1.

From simulations the photon energy resolution for FoCal is estimated to be $\sigma_E = 25\%/\sqrt{E} \oplus 2\%$. This is comparable to that expected for the sPHENIX W/SciFi calorimeter. Other technologies that would provide suitable resolution include crystals ($PbWO_4$, LYSO, GSO, LSO), DSB:Ce glass, and W/SciFi. $PbWO_4$ crystals and DSB:Ce glass have been developed and characterized by the eRD1 Consortium and the Neutral Particle Spectrometer project at Jefferson Lab. Tests have shown energy resolutions of $\sim 2\%/\sqrt{E}$ for photon energies ~ 4 GeV [29].

To identify neutrons, the ZDC needs a hadronic section with a resolution of $\sigma_E < 50\%/\sqrt{E}$ with an angular resolution of at least 3 mrad / $\sqrt{E}$ is desired. Cerenkov calorimeters, which measure only the high energy component of the showers, give excellent position resolution and tight containment but are non-compensating and so somewhat non-linear. Sampling all charged particles produced gives better energy resolution at the cost of worse lateral containment. We seek to exploit both techniques to maximize both the energy and

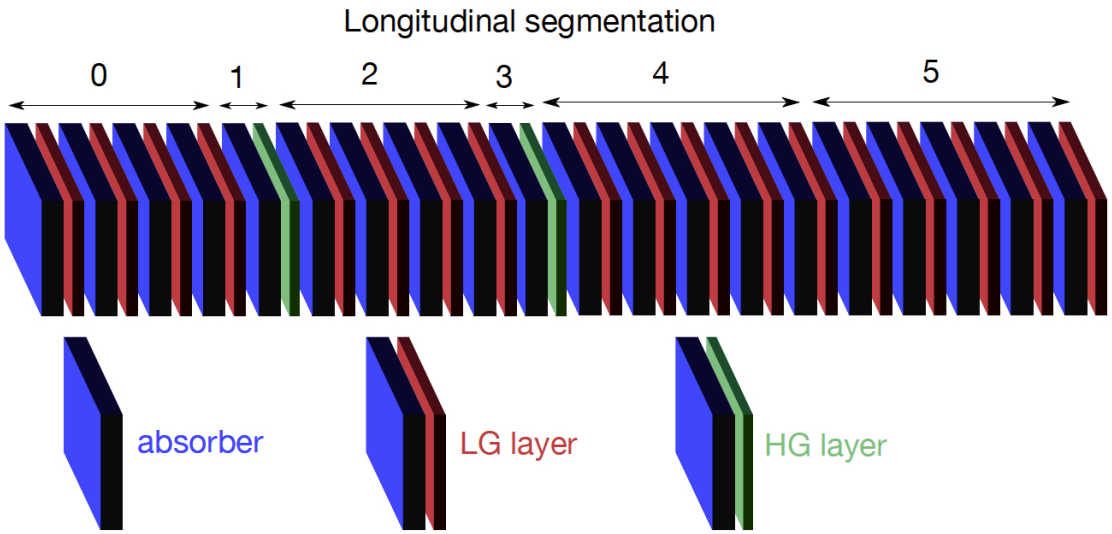

Figure 14.1: Schematic of the FoCal electromagnetic calorimeter. The blue absorber is tungsten, the red low granularity silicon layers are used for energy measurement while the green high granularity layers give precise position information [28].

position resolution of the ZDC. This could be done by using the quartz fibers developed for the LHC ZDCs, [30], with traditional scintillators.

In order to detect coherent collisions it is necessary to veto events in which soft photons are emmitted from an excited nucleus For ^{208}Pb, every bound-state decay sequence has at least one photon with an energy of at least 2.6 MeV. For a beam momentum of 275 GeV/c, 20% of these decay photons (with minimum energy 455 MeV) are detectable in the ZDC aperture of $\sim$ 4.5 mrad. In order to detect such photons from nuclear excitation it is important that the ZDC have the largest possible aperture. It is possible that a 2nd IR design will allow a larger ZDC acceptance.

The meson structure research for the EIC has shown the need of a tracker, in combination with the ZDC, to be used as a veto detector for π^- for an efficient measurement of the $\Lambda \rightarrow n + \pi^0$ channel. Besides this main purpose, adding a tracker could improve the reconstruction of charged particles in the ZDC for other different channels. A non-expensive and feasible option is the use of scintillating fibers (SciFi) as a tracker detector.

The number of spectator neutrons is predicted to have somewhat correlation with the collision geometry. The required performance of the detector to identify the coherence of the collision is under development using the BeAGLE simulation [31]. Some of performance parameters are under ongoing study. The optimization of the performance requirements is included in the scope of the development based on the requirements known as of now as listed below.

A large acceptance (e.g. 60×60 cm^2) to establish good identification efficiency between coherent and incoherent collisions is necessary for vetoing spectator neutrons from nuclear

breakup. This large acceptance is also required to determine the collision geometry [32] . For studying very forward production and asymmetry of hadrons and photons, a large acceptance is also important. The EIC aperture of ± 4 mrad gives $p_T < 1\text{GeV}/c$ coverage for 275 GeV hadrons and photons, which covers the transition from elastic/diffraction to incoherent regime; for low-energy hadron beam the acceptance in terms of p_T is more limited e.g. $p_T < 0.4\text{GeV}/c$ coverage for 100 GeV beam.

Due to the strong β squeeze < 1 meter for the high luminosity, a beam spread of $\sim$20 MeV and $\sim$1 cm of the hadron beam angular divergence is induced. Thus the position resolution of neutron in sub cm won't help. 1 cm position resolution provides 300 μrad angular resolution, which can be translated to transverse momentum resolution $p_{\mathrm{T}} \sim 30$ MeV/c of 100 GeV spectator neutron.

The minimum energy resolution $\Delta E/E \sim 50\%/\sqrt{E(GeV)}$ to distinguish number of spectator neutrons from 20 to 30 for collision geometry determination. In order to accommodate a single MIP track to 30 spectator neutrons, wide dynamic energy range in the readout electronics is required.

It is anticipated to be a sampling type calorimeter with a sufficient longitudinal size of $\sim$10 interaction length [32]. It is also required to have a sufficient transverse size of $\sim$2 interaction length to avoid transverse leakage of the hadron shower and to achieve good hadron energy resolution.

14.5.3 Superconducting-Nanowire Particle Detectors

Superconducting Nanowire Single-Photon Detectors (SNSPDs) have become the dominant technology in quantum optics due to their unparalleled timing resolution and quantum efficiency. The Argonne National Laboratory group, supported by eRD28, is currently investigating the pathway to transform these sensors into a novel particle detector for the EIC. The sensors can operate in magnetic fields greater than 5 T at a high rate with high efficiency, and with a timing resolution as low as $\lesssim$ 20 ps. The R&D effort aims to produce a small (mm^2) superconducting nanowire pixel array for detecting high energy particles. This first of its kind detector will have the flexibility to be used in multiple far forward detector systems. It can extend the EIC's scientific reach beyond what is possible with contemporary technology for far-forward detection.

Superconducting nanowire detectors have multiple characteristics that make them a uniquely capable detector technology for applications at the EIC. (a) Superconducting nanowire detectors are high-speed detectors and have time resolutions typically on the order of 20 ps scale, with a current record of 3 ps. (b) A meandering wire layout allows for small pixel sizes and allows for µm position resolution if needed. (c) Single pixels can operate efficiently at high-rates in strong magnetic fields (up to 5 T) [33]. (d) Edgeless sensor configurations are a possibility, with the sensitive element positioned to within a few 100 nm of the substrate edge, eliminating dead material in between the particle beam and the detector. (e) Wide choice of substrate material – the detectors can be fabricated on membranes as thin as few 10 µm, further cutting down on material thickness. (f) Radia-

tion hardness allows for a longer service cycle of detectors operating near the beam and interaction regions.

The EIC R&D committee identified four applications at the EIC for future R&D [34]. (1) A Roman pot detector in the forward region about 35 meters or more from the interaction point to tag low momentum transfer recoiling ions. (2) An integrated detector inside the cold bore of superconducting magnets for the forward ion detection would provide tracking in regions of high magnetic fields. This would include placing the detector inside the magnet and integrating it with the magnet's cooling system, eliminating the need for a separate cryogenic system. Further applications include (3) placing the detector in front of the ZDC detector and around the forward ion spectrometer section, filling in the detection gaps where radiation hard detectors with excellent position and timing resolution are needed. Finally, (4) use in an electron detector for a Compton Polarimeter, because the high rate capability, allows the nanowire detectors to handle the 100 MHz beam pulse rate to measure the azimuthal asymmetries needed to extract the beam polarization.

Superconducting nanowire sensors are an entirely new technology for high energy particle detection in nuclear physics [35]. This unique opportunity comes with some R&D needs to leverage the full potential for applications at the EIC. Further R&D includes optimizing the wire parameters or high energy ion detection, developing cryogenic bias and readout ASICs for high channel count tracking detectors, and design integration of superconducting nanowire sensors into the cold bore of superconducting magnets. The required R&D can be completed within the next few years, depending on the specific application.

14.6 Data Acquisition

14.6.1 Streaming-Capable Front-End Electronics, Data Aggregation, and Timing Distribution

A streaming readout is the likely readout paradigm for the EIC, as it allows easy scaling to the requirements of EIC, enables recording more physics more efficiently, and allows better online monitoring capabilities. The EIC detectors will likely be highly segmented, leading to a large number of readout channels. At the same time, multiplicities and pile-up are likely less demanding than other experiments like sPHENIX. The physics case is very wide, and many analysis will be systematics dominated. It is therefore crucial to minimize systematic effects from the readout, for example trigger biases. Further, minimally biased data recording allows to data-mine for novel physics later in the EIC life-cycle. A streaming readout system further reduces scaling choke-points and critical failure points like online event building.

A working readout system is crucial for any data taking and must be ready at day-1. In fact, ideally, prototypes should be ready for detector tests well ahead of first beam. R&D is required in multiple areas: Streaming readout requires the distribution of clock information. While crucial for successful data taking, this is a less demanding task than the distribution of triggers, and a scheme similar to the one at sPHENIX is a likely solution.

This approach will be tested by sPHENIX well ahead of EIC completion, and other test beams will likely use other timing systems. Front end electronics need to be read out via some sort of data collection hardware. These will likely be evolutions of already available components like the FELIX cards, and existing hardware can be used during test beams until the final hardware iterations are available. Both of these research topics are rather low risk.

Of higher risk is the development of suitable front-end electronics. Here, possible front-end readout ASICs have to be matched to the detector requirements. While existing ASICs cover many use cases, it is not clear yet if the requirements of the final detector configurations for the EIC are covered by current capabilities. History tells us that timelines for development of completely new ASICs is 6 or more years, while modifications of existing designs might be done in 3+ years. It is therefore paramount that cases where new readout ASICs are required are identified soon, and whether a readout is at all feasible within the given constraints. This puts this research into the high-risk and high priority category. We want to note here that this risk is not unique to a streaming readout—in fact, most high-performance ASICs today fit a streaming readout solution better than a triggered one—and is indeed a risk for the readout in general, independent of chosen paradigm.

The research intrinsically touches upon a wide range of other detector projects. It is very likely that data collection hardware is shared between most detector components. For front-end electronics, designs will be shared as much as possible.

14.6.2 Readout Software Architecture, Orchestration and Online Analysis

COMMENT-TU: Missing connection to R&D... JCB: I think I addressed it. Please check.

In addition to readout hardware, it is important to develop and test protocols and software to provide a stable, high-performing readout. This includes a scalable platform, both in channel count and processing capabilities, and the inclusion of analysis into the online system as much as possible. The system must be resilient against errors in the FEE to enable an overall highly efficient data taking. High quality, high level monitoring will secure the recording of high-quality data, reducing time-to-publication. Similar to the hardware, prototype designs should be ready well in advance to support test beam times, and to collect experience necessary to build the online analysis.

The development of software and protocol components must go hand in hand with the hardware. As the highest priority, it is important to define a logical protocol for data exchange. This will enable groups to develop interoperable electronics and software components early in the development cycle. The community is actively working on this issue, but revisions will be likely in the years to come.

To achieve optimal usage of beam times, techniques must be developed to make the readout resilient against FEE errors (e.g. Single Event Upsets) without requiring a full stop and restart of the system. This issue is exacerbated by the high channel count and density. In a similar fashion, it is an open research question how to best address bandwidth restrictions.

Since the data rate is governed by a stochastic process, they will have peak rates substantially above the average data rate, with almost no ceiling. While large memory buffers can mitigate this by smearing out peak rates over time, the system must still be able to handle buffer overflows. For both problems, R&D is required to develop a framework and control algorithms that react in a predictable and reconstructable way, so that overall detector/DAQ efficiencies can be extracted. Such a system must be available essentially at first beam, with improvements later in the life cycle.

The amount of data collected and the changing landscape of compute infrastructure to a federated model makes it necessarily to rethink data storage and retrieval to achieve efficient usage of the computing resources. Here, a flexible software layer must be developed to isolate the analysis code from the changing infrastructure. While a first solution is required at first beam, it is likely that this will evolve together with the compute infrastructure during the EIC lifecycle. Connected to this issue is the integration of analysis into the online and near-online processing to maximize data quality. This includes the efficient handling of calibration procedures, and minimization of time delay between analysis and data taking.

The latter points are, to some degree, also required R&D for other projects like sPHENIX and CLAS-12, and an EIC solution would likely be straight-forward iterative development. On the other hand, even with sophisticated simulations and detector tests, the initial conditions at an EIC in the sense of observed background and dark rates, beam quality etc. are hard to predict, and will probably require some time for tuning. The initial rates might overwhelm the readout system and a system to mitigate this risk must be developed. A possible avenue is include a hard data reduction stage early in the readout system, for example controlled by a trigger, or via software cuts at a very early stage. This capability is the equivalent of raising trigger thresholds or disabling trigger sources in a classical triggered system, and would secure the ability to record data required to understand and calibrate detectors and optimize the machine, at the cost of physics reach during this tune-up period. A possible approach based on hardware signals is essentially realized at sPHENIX, and other implementations are straight forward. Research and development has to show if a pure software-based solution can be implemented, which would allow for more flexibility in the transition to normal operation.

14.7 Electronics

14.7.1 R&D of High Precision Timing Distribution Over Large System

High precision timing distribution is important for sub-detectors like TOF and LGAD based timing detectors. This technology will be used to distribute phase controllable high precision clocks to sub-detectors, and to provide precision timing for the physics events. It should also support online calibration of the clock phase drift caused by fluctuation of the environment, for instance the temperature drift. As a reference, for proposed TOF in sPHENIX and LGAD detectors in HL-LHC, the required resolution for measurements of

individual arrival times of particles is about 25 to 50 ps, to mitigate the relatively short flight length, the extreme pile-up and occupancy [36]. The contribution of the resolution comes from both detector and electronics. For future HEP experiments, the requirement to the electronics may reach picosecond level. R&D based on phase adjustment and measurement within the back-end FPGA is a candidate solution for it. The R&D will focus on the back-end electronics in the DAQ system and the front-end readout electronics of sub-detectors. It will demonstrate the full path of transmission of signal and data with the system clock embedded. The most critical part of the R&D is to guarantee the phase stability of the low jitter clock in the front-end. Leverage of expertise is available in ongoing R&D at CERN for HL-LHC experiments [37]. Depending on the detailed requirements of EIC, this R&D may be finished in about 1 year.

14.7.2 R&D of FPGA Operation in Radiation Environment

Depending on the design methodology for the sub-detectors readout electronics, FPGAs may be used in the FEB (front-end board) and FEP (front-end processor) board. Both will have to endure radiation, especially for the FEB board. This R&D will mainly focus on the application of commercial FPGAs in the front-end electronics. The purpose is to provide common FPGA based solutions for readout electronics in a radiation environment. Some similar research has been carried out for existing FPGAs, for example the Xilinx 7 series and Ultrascale series FPGAs in sPHENIX and the LHC experiments. This R&D will focus on: selection of the FPGA (SRAM-based or Flash-based FPGA) depending on the detailed requirements to the FPGA functions, radiation dose and radiation types; the measurement of cross section for different types of errors caused by the radiation; and the FPGA firmware design methodology to mitigate the errors like SEU and SEFI, for example the TMR (Triple Modular Redundancy) for the logic firmware, the data coding with error correction for high-speed serial links and the scrubbing for FPGA configuration. Several radiation tests will be needed for this R&D. The whole R&D may last for 1 to 1.5 years and will inform the selection criteria, as well as, implementation mitigating factors.

14.7.3 R&D of Micro-electronics, Optop-electronics and Powering

R&D of Micro-electronics will include survey and evaluation of CMOS technologies such as 65nm, 28nm technologies; facilitate the mitigation of radiation effects on the technology; models, cell libraries and IP blocks development for extreme environments [36, 38]. Due to the limited available resources within the EIC community, expertise and experience from HEP should be employed. R&D of specific front-end ASICs will depend on the requirements from the various sub-detectors.

R&D of Opto-electronics: this is mainly about the radiation hard optical link architecture for high speed serial links, including the optical module and common ASIC for data aggregation [38]. This R&D may need a lot of effort, but the existing designs with 2.5 Gbps, 5 Gbps and 10 Gbps line rate at CERN for LHC and HL-LHC experiments [39] should be

competent for EIC. Small revisions may be needed to match with the EIC machine parameters, for instance different clock frequency and line rate for the data transmission.

R&D of powering may need to cover: research on radiation tolerant DC-DC converters, for instance the development activities at CERN [40]; low voltage power distribution; serial powering for trackers.

For readout and data acquisition, it would be critical for its R&D to be integrated with the detector technology selection, design and prototyping. The detector groups are encouraged to work closely with the readout and DAQ group in considering readout requirements (e.g. noise performance requirement), using the supported readout chips (e.g. streaming compatible chips), and perform tests with the compatible DAQ software (RCDAQ, etc.) at the earliest opportunities.

Appendix A

Deep Inelastic Scattering Kinematics

A.1 Structure functions

In general, the inclusive DIS process can be written as

$$e(l) + N(p) \rightarrow e(l') + X(p_X), \tag{A.1}$$

where e refers to the electron or positron, N is the nucleon in the initial state with momentum p, and a system X (which is not measured) is produced with momentum p_X. In case of an unpolarized nucleon, the cross section for this process can be written in terms of the structure functions F_2 and F_L in the one photon exchange approximation neglecting electroweak effects as

$$\frac{\mathrm{d}\sigma}{\mathrm{d}x\mathrm{d}Q^2} = \frac{4\pi\alpha^2}{xQ^4}\left[\left(1 - y + \frac{y^2}{2}\right)F_2(x,Q^2) - \frac{y^2}{2}F_L(x,Q^2)\right]. \tag{A.2}$$

Instead of structure functions, the reduced cross section σ_r is often used

$$\sigma_r = \frac{\mathrm{d}^2\sigma}{\mathrm{d}x\mathrm{d}Q^2}\frac{xQ^4}{2\pi\alpha^2[1+(1-y)^2]} = F_2(x,Q^2) - \frac{y^2}{1+(1-y)^2}F_L(x,Q^2). \tag{A.3}$$

With longitudinally polarized electron and nucleon beams, it is also possible to extract the structure function g_1

$$\frac{1}{2}\left[\frac{\mathrm{d}\sigma^{\rightleftarrows}}{\mathrm{d}x\mathrm{d}Q^2} - \frac{\mathrm{d}\sigma^{\rightrightarrows}}{\mathrm{d}x\mathrm{d}Q^2}\right] = \frac{4\pi\alpha^2}{Q^4}y(2-y)g_1(x,Q^2). \tag{A.4}$$

Here terms suppressed by $x^2m_N^2/Q^2$ have been neglected, and $\sigma^{\rightleftarrows}$ refers to the case where the nucleon and electron spins are opposite (and parallel to the z axis), and $\sigma^{\rightrightarrows}$ to the scattering process in case of aligned spins. The kinematical variables x,y and Q^2 are introduced below, and m_N is the nucleon mass and α is the fine structure constant. At large Q^2 and to leading order in the strong coupling constant α_s the F_2 structure function is proportional

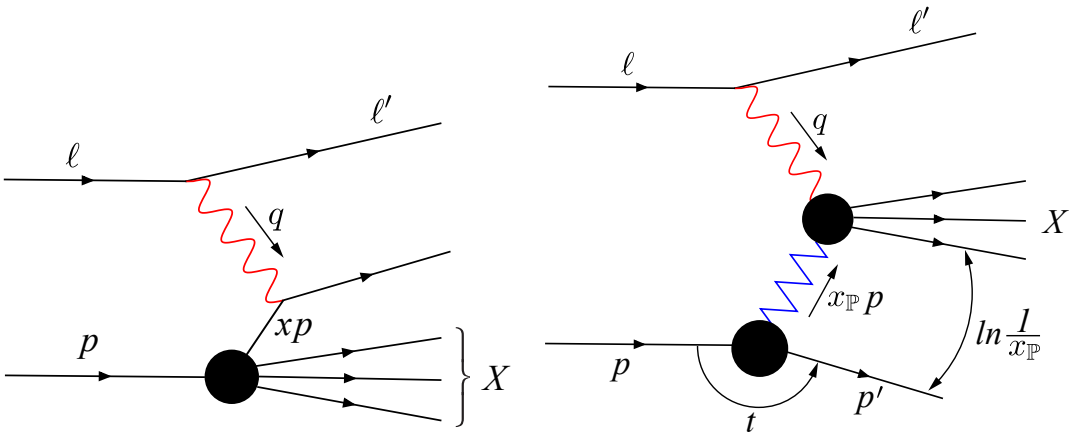

(a) Inclusive DIS **(b)** Diffractive scattering

Figure A.1: Kinematical variables of inclusive and exclusive DIS. The blobs correspond to interactions.

to the unpolarized quark and antiquark distributions in the nucleon, and g_1 is sensitive to the longitudinally polarized distributions. In this limit $F_L = 0$, and it obtains a first contribution at next to leading order in perturbative expansion, and is thus particularly sensitive to the gluon distribution.

In diffractive (and also semi-inclusive) scattering, the process becomes

$$e(l) + N(p) \rightarrow e(l') + N'(p') + X(p_X), \tag{A.5}$$

where N' refers to the nucleon or the nucleon remnants in the final state with momentum p' and a specific system X is produced. The electron mass is neglected in the following discussion, and the nucleon mass $p^2 = m_N^2$ is kept non-zero unless otherwise stated. In this appendix, p is a four vector and $\mathbf{p}$ and $\mathbf{p}_\perp$ refer to the three-momentum and the transverse momentum, respectively. The momentum vectors are illustrated in Fig. A.1.

A.2 Invariants

Let us first consider inclusive scattering where the final state X is not completely determined and the scattered nucleon (nucelon remnants) are not reconstructed. The center-of-mass energy squared for the DIS process can be written using the momenta defined in Eq. (A.1) as

$$s = (l + p)^2 = m_N^2 + 2p \cdot l \approx 2\sqrt{E_e E_n}. \tag{A.6}$$

Here E_e is the electron energy and E_n the nucleon energy, and the approximation is valid in the high energy limit where the nucleon mass can be neglected.

As the scattering process is mediated by a virtual photon, the center-of-mass energy W for

the photon-nucleon system is generically more useful:

$$W^2 = (p+q)^2 = m_N^2 - Q^2 + 2p\cdot q. \tag{A.7}$$

Here the virtual photon momentum is $q = l - l'$ and its virtuality $-Q^2 = (l-l')^2$. The other useful Lorentz invariant quantities describing the DIS process are

$$x \equiv \frac{Q^2}{2p\cdot q} = \frac{Q^2}{2m_N\nu} = \frac{Q^2}{Q^2 + W^2 - m_N^2} \tag{A.8}$$

$$y \equiv \frac{p\cdot q}{p\cdot \ell} = \frac{W^2 + Q^2 - m_N^2}{s - m_N^2} \tag{A.9}$$

These invariants have intuitive physical interpretations in particular frames. The Bjorken variable x can be interpreted in the parton model in the infinite momentum frame where the nucleon carries a large longitudinal momentum. In such a frame, x is the fraction of the nucleon momentum carried by the stuck parton if the quark masses are neglected. In electron-nucleon collisions, $0 < x < 1$.

The variable y is called *inelasticity*. When expressed in the nucleon rest frame, one finds $y = 1 - \frac{E_l'}{E_l}$, where E_l and E_l' are the energies of the incoming and outgoing leptons in this frame, respectively. Consequently, $0 \leq y \leq 1$, and in particular, the highest possible photon-nucleon center-of-mass energies are reached at the $y \to 1$ limit. A closely related variable ν also exists: $\nu \equiv \frac{p\cdot q}{m_N}$ describes, in the nucleon rest frame, the electron energy carried away by the virtual photon: $\nu = E_l - E_{l'}$.

The invariants presented above are not independent, and in inclusive scattering the collision kinematics is completely determined by three variables, e.g. s, Q^2 and x. This becomes apparent when noticing that the invariants defined above satisfy e.g. the following relations:

$$Q^2 = xy(s - m_N^2), \text{ and} \tag{A.10}$$

$$W^2 = \frac{1-x}{x}Q^2 + m_N^2. \tag{A.11}$$

The smallest kinematically allowed virtuality Q^2_{min} can be determined if the electron mass m_e is non-zero: $Q^2_{\text{min}} = m_e^2\frac{y^2}{1-y}$.

Let us then discuss diffractive production of a system X with an invariant mass M_X^2. In the unpolarized case where the cross section is symmetric in azimuthal angle, we can describe the kinematics by introducing the following new invariants:

$$t \equiv -(p'-p)^2 \tag{A.12}$$

$$x_{\mathbb{P}} \equiv \frac{(p-p')\cdot q}{p\cdot q} = \frac{M_X^2 + Q^2 - t}{W^2 + Q^2 - m_N^2} \tag{A.13}$$

$$\beta \equiv \frac{Q^2}{2q \cdot (p - p')} = \frac{Q^2}{M_X^2 + Q^2 - t} \tag{A.14}$$

In the infinite momentum frame, $x_{\mathbb{P}}$ has the interpretation that in the scattering process an exchange of vacuum quantum numbers (a *pomeron* exchange) takes place, and the pomeron carries a fraction of $x_{\mathbb{P}}$ of the nucleon longitudinal momentum. Similarly, in the partonic language β is the longitudinal momentum of the struck parton inside the pomeron. These invariants are not independent, and can be related to the invariants of inclusive DIS discussed above via e.g.

$$x = \beta x_{\mathbb{P}}. \tag{A.15}$$

An experimental signature of a diffractive event is the presence of a rapidity gap between the outgoing nucleon (nucleon remnants) and the system X. This gap size is $\Delta y \sim \ln 1/x_{\mathbb{P}}$.

A.3 Laboratory frame

In the laboratory frame the collisions are asymmetric, and the inclusive DIS invariants can be determined by measuring the energy and the scattering angle of the outgoing electron. In the limit of small nucleon mass, the invariants read

$$s = 4E_e E_n \tag{A.16}$$

$$Q^2 = 2E_e E_e'(1 - \cos\theta_e) \tag{A.17}$$

$$W^2 = 4E_e E_n - 2E_e' \left[E_n + E_e + (E_n - E_e)\cos\theta_e\right] \tag{A.18}$$

$$x = \frac{E_e E_e'(1 - \cos\theta_e)}{2E_e E_n - E_e' E_n(1 + \cos\theta_e)} \tag{A.19}$$

$$y = \frac{2E_e E_n - E_e' E_n(1 + \cos\theta_e)}{2E_e E_n}. \tag{A.20}$$

Here E_e and E_e' are the incoming and outgoing electron energies, and the electron scattering angle is θ_e, with $\theta_e = 0$ corresponding to the forward scattering, or photoproduction region $Q^2 \approx 0$. Similarly the incoming nucleon energy is E_n.

In exclusive processes it is possible to also measure the momentum of the produced particle and its invariant mass by measuring the decay products. Although the kinematical variables can be reconstructed using the scattered electron only, a common method to determine y and Q^2 is to express these invariants in terms of the scattering angles of both the electron and the produced particle using the double angle method [41]:

$$Q^2 = 4E_e^2 \frac{\sin\theta_e(1 - \cos\theta_V)}{\sin\theta_V + \sin\theta_e - \sin(\theta_e + \theta_V)} \tag{A.21}$$

$$y = \frac{\sin\theta_e(1 - \cos\theta_V)}{\sin\theta_V + \sin\theta_e - \sin(\theta_e + \theta_V)}. \tag{A.22}$$

Here θ_V is the scattering angle of the produced particle. These expressions are again valid in the limit where the nucleon mass can be neglected, and other similar methods can be found from Ref. [41]. Note that once Q^2 and y are determined, x and W^2 can be obtained using Eqs. (A.10) and (A.11).

The squared momentum transfer t can be written as

$$t = -\frac{(\mathbf{p_X}_\perp - \mathbf{l'}_\perp)^2 + x_{\mathbb{P}}^2 m_N^2}{1 - x_{\mathbb{P}}} \approx -(\mathbf{p_X}_\perp - \mathbf{l'}_\perp)^2. \tag{A.23}$$

Here $\mathbf{p_X}_\perp$ is the transverse momentum of the produced particle and $\mathbf{l'}_\perp$ the transverse momentum of the scattered electron, and the approximation is valid at high energies where $x_{\mathbb{P}}$ is small and the momentum transfer is approximatively transverse. Note that the kinematical lower bound for t reads

$$-t > -t_{\min} = \frac{x_{\mathbb{P}}^2 m_N^2}{1 - x_{\mathbb{P}}}. \tag{A.24}$$

When t, Q^2 and W^2 are determined, $x_{\mathbb{P}}$ can be obtained by using Eq. (A.13).

In exclusive and semi-inclusive processes the particle X is identified by measuring the invariant mass of the decay products. In inclusive diffraction the invariant mass M_X^2 is determined by measuring the total energy E_X and the total momentum $\mathbf{p_X}$ of the produced particles:

$$M_X^2 = E_X^2 - \mathbf{p_X}^2. \tag{A.25}$$

In these events, it is also possible to construct inelasticity using the hadron method

$$y_h = \frac{E_X - \mathbf{p_X}_z}{2E_e}. \tag{A.26}$$

The hadron method can also be used to determine inelasticity in exclusive particle production in the photoproduction limit where the scattered electron can not be detected. For a better experimental accuracy, different methods to construct e.g. inenalasticity can be combined (see e.g. [42]). Generically in inclusive diffraction $M_X^2 + Q^2 \gg |t|$, and consequently t can be neglected when determining $x_{\mathbb{P}}$ and β using Eqs. (A.13) and (A.14).

A.4 Breit frame

A natural frame to describe hard scattering process in DIS is the Breit (or brick wall) frame, where the incoming photon carries no energy, and the parton to which the photon couples to behaves as if it bounced off a brick wall. Let us choose that the ultrarelativistic nucleon moves along the positive z axis, and the photon propagates to the $-z$ direction. The nucleon momentum in this frame is $p_z = \frac{1}{2x}Q$, and the parton longitudinal momentum k_z can be written as $k_z = xp_z = \frac{1}{2}Q$. Similarly, the photon four-momentum reads $q = (0, 0, 0, -Q)$. Now, after the photon absorption $\mathbf{k}' = -\mathbf{k}$, where $\mathbf{k}'$ is the parton mo-

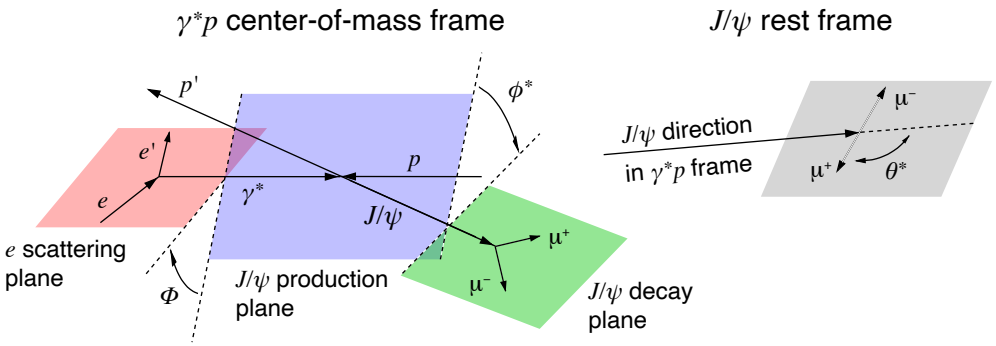

Figure A.2: Planes in exlcusive vector meson production.

mentum after the scattering. Note that in this frame there is no energy transfer to the proton.

The Breit frame is not the center-of-mass frame for the parton-photon scattering. This is advantageous when separating the produced particles from the beam remnants. In the Breit frame, the produced particles populate the region of negative z momentum, while the beam remnants generically have a positive momentum z component.

A.5 Helicity studies

Studying the helicity structure of exclusive particle production processes requires one to measure the azimuthal angles ϕ^* and Φ defined in Fig. A.2. Note that the angles are defined in the frame where the photon and the nucleon momenta are aligned along the same axis (here z axis), so this discussion is valid both in the Breit frame and in the γ-nucleon center-of-mass frame.

The production plane is defined as the plane spanned by the z axis and the momentum of the produced particle. The azimuthal angle between this plane, and the electron scattering plane spanned by the momenta of the incoming and outoing electron momentum vectors is denoted by Φ in Fig. A.2, where the geometry is illustrated in case of $e^+ + p \to e^+ + p +$ J/ψ scattering. Similarly, we define the decay plane, which is spanned by the momenta of the decay products of the prodcued particle, and the azimuthal angle between this plane and the production plane is denoted by ϕ^*.

The third angle required to specify the geometry θ^* also shown in Fig. A.2 is required to determine the polarization state of the produced particle. This angle is defined as the polar angle of the decay particle having the same charge as the incoming lepton in the rest frame of the decaying particle. The $\theta^* = 0$ case corresponds to the direction of the produced particle in the photon-nucleon center-of-mass frame.

References

[1] G. Pellegrini *et al.*, "Technology developments and first measurements of low gain avalanche detectors (LGAD) for high energy physics applications," *Nuclear Instruments and Methods in Physics Research Section A: Accelerators, Spectrometers, Detectors and Associated Equipment*, vol. 765, pp. 12 – 16, 2014. HSTD-9 2013 - Proceedings of the 9th International Hiroshima Symposium on Development and Application of Semiconductor Tracking Detectors.

[2] R. Padilla, C. Labitan, Z. Galloway, C. Gee, S. Mazza, F. McKinney-Martinez, H.-W. Sadrozinski, A. Seiden, B. Schumm, M. Wilder, Y. Zhao, H. Ren, Y. Jin, M. Lockerby, V. Cindro, G. Kramberger, I. Mandiz, M. Mikuz, M. Zavrtanik, R. Arcidiacono, N. Cartiglia, M. Ferrero, M. Mandurrino, V. Sola, and A. Staiano, "Effect of deep gain layer and carbon infusion on LGAD radiation hardness," *Journal of Instrumentation*, vol. 15, pp. P10003–P10003, oct 2020.

[3] Y. Jin *et al.*, "Experimental study of acceptor removal in UFSD," *Nuclear Instruments and Methods in Physics Research Section A: Accelerators, Spectrometers, Detectors and Associated Equipment*, vol. 983, p. 164611, Dec 2020.

[4] N. Cartiglia, A. Staiano, V. Sola, R. Arcidiacono, R. Cirio, F. Cenna, M. Ferrero, V. Monaco, R. Mulargia, M. Obertino, F. Ravera, R. Sacchi, A. Bellora, S. Durando, M. Mandurrino, N. Minafra, V. Fadeyev, P. Freeman, Z. Galloway, E. Gkougkousis, H. Grabas, B. Gruey, C. Labitan, R. Losakul, Z. Luce, F. McKinney-Martinez, H.-W. Sadrozinski, A. Seiden, E. Spencer, M. Wilder, N. Woods, A. Zatserklyaniy, G. Pellegrini, S. Hidalgo, M. Carulla, D. Flores, A. Merlos, D. Quirion, V. Cindro, G. Kramberger, I. Mandić, M. Mikuž, and M. Zavrtanik, "Beam test results of a 16ps timing system based on ultra-fast silicon detectors," *Nuclear Instruments and Methods in Physics Research Section A: Accelerators, Spectrometers, Detectors and Associated Equipment*, vol. 850, pp. 83 – 88, 2017.

[5] A. Apresyan, W. Chen, G. D'Amen, K. F. Di Petrillo, G. Giacomini, R. Heller, H. Lee, S. Los, C.-S. Moon, and A. Tricoli, "Measurements of an AC-LGAD strip sensor with a 120 GeV proton beam," *JINST*, vol. 15, no. 09, p. P09038, 2020.

[6] H. Pernegger *et al.*, "First tests of a novel radiation hard CMOS sensor process for depleted monolithic active pixel sensors," *Journal of Instrumentation*, vol. 12, pp. P06008–P06008, jun 2017.

[7] I. Berdalovic *et al.*, "Monolithic pixel development in towerjazz 180 nm cmos for the outer pixel layers in the atlas experiment," *JINST*, vol. 13, p. C C01023, 2018.

[8] B. Hiti *et al.*, "Development of the monolithic "MALTA" CMOS sensor for the ATLAS ITK outer pixel layer," *PoS*, vol. TWEPP2018, p. 155, 2019.

[9] R. Schimassek, A. Andreazza, H. Augustin, M. Barbero, M. Benoit, F. Ehrler, G. Iacobucci, A. Meneses, P. Pangaud, M. Prathapan, A. Schöning, E. Vilella, A. Weber, M. Weber, W. Wong, H. Zhang, and I. Perić, "Test results of ATLASPIX3 — a reticle size HVCMOS pixel sensor designed for construction of multi chip modules," *Nuclear Instruments and Methods in Physics Research Section A: Accelerators, Spectrometers, Detectors and Associated Equipment*, vol. 986, p. 164812, 2021.

[10] L. Barion *et al.*, "RICH detectors development for hadron identification at EIC: design, prototyping and reconstruction algorithm," *JINST*, vol. 15, no. 02, p. C02040, 2020.

[11] E. Cisbani *et al.*, "AI-optimized detector design for the future Electron-Ion Collider: the dual-radiator RICH case," *JINST*, vol. 15, no. 05, p. P05009, 2020.

[12] W. Anderson *et al.*, "Design, Construction, Operation and Performance of a Hadron Blind Detector for the PHENIX Experiment," *Nucl. Instrum. Meth. A*, vol. 646, pp. 35–58, 2011.

[13] J. Agarwala *et al.*, "The MPGD-Based Photon Detectors for the upgrade of COMPASS RICH-1 and beyond," *Nucl. Instrum. Meth. A*, vol. 936, pp. 416–419, 2019.

[14] M. Blatnik *et al.*, "Performance of a Quintuple-GEM Based RICH Detector Prototype," *IEEE Trans. Nucl. Sci.*, vol. 62, no. 6, pp. 3256–3264, 2015.

[15] B. Azmoun *et al.*, "Results from a Prototype Combination TPC Cherenkov Detector with GEM Readout," *IEEE Trans. Nucl. Sci.*, vol. 66, no. 8, pp. 1984–1992, 2019.

[16] S. N. White, "R&D for a Dedicated Fast Timing Layer in the CMS Endcap Upgrade," *Acta Phys. Pol. B Proc. Suppl.*, vol. 7, p. 743, 2014.

[17] N. Cartiglia *et al.*, "Design optimization of ultra-fast silicon detectors," *Nucl. Instrum. Meth. A*, vol. 796, p. 141, 2015.

[18] D. Breton *et al.*, "Measurements of timing resolution of ultra-fast silicon detectors with the SAMPIC waveform digitizer," *Nucl. Instrum. Meth. A*, vol. 835, p. 51, 2016.

[19] N. Minafra *et al.*, "Test of Ultra Fast Silicon Detectors for Picosecond Time Measurements with a New Multipurpose Read-Out Board," *Nucl. Instrum. Meth. A*, vol. 867, p. 88, 2017.

[20] A. Apresyan *et al.*, "Studies of Uniformity of 50 μm Low-Gain Avalanche Detectors at the Fermilab Test Beam," *Nucl. Instrum. Meth. A*, vol. 895, p. 158, 2018.

[21] C. Collaboration, "A MIP Timing Detector for the CMS Phase-2 Upgrade," Tech. Rep. CERN-LHCC-2019-003. CMS-TDR-020, CERN, Geneva, 3 2019.

[22] A. Collaboration, "Technical Proposal: A High-Granularity Timing Detector for the ATLAS Phase-II Upgrade," Tech. Rep. CERN-LHCC-2018-023. LHCC-P-012, CERN, Geneva, 6 2018.

[23] M. Jadhav, W. Armstrong, I. Cloet, S. Joosten, S. Mazza, J. Metcalfe, Z.-E. Meziani, H. Sadrozinski, B. Schumm, and A. Seiden, "Picosecond Timing Resolution Measurements of Low Gain Avalanche Detectors with a 120 GeV Proton Beam for the TOP-SiDE Detector Concept," 2020.

[24] O. Tsai *et al.*, "Development of a forward calorimeter system for the STAR experiment," *J. Phys. Conf. Ser.*, vol. 587, no. 1, p. 012053, 2015.

[25] C. Aidala *et al.*, "Design and Beam Test Results for the sPHENIX Electromagnetic and Hadronic Calorimeter Prototypes," *IEEE Trans. Nucl. Sci.*, vol. 65, no. 12, pp. 2901–2919, 2018.

[26] O. Tsai *et al.*, "Results of \& on a new construction technique for W/ScFi Calorimeters," *J. Phys. Conf. Ser.*, vol. 404, p. 012023, 2012.

[27] S. Trentalange *et al.*, "T-1018: UCLA Spacordion Tungsten Powder Calorimeter," tech. rep., Fermilab, 12 2013.

[28] A. Collaboration, "A Forward Calorimeter (FoCal) in the ALICE experiment," tech. rep., CERN, Oct 2019.

[29] T. Horn, "A $PbWO_4$-based Neutral Particle Spectrometer in Hall C at 12 GeV JLab," *J. Phys. Conf. Ser.*, vol. 587, no. 1, p. 012048, 2015.

[30] "Joint Zero Degree Calorimeter Project." `http://jzcap.physics.illinois.edu/pages.html`.

[31] Aschenauer, E.C. and Baker, M.D. and Lee, J.H. and Zheng, L., "EIC R&D Project eRD17 Progress Report." `https://wiki.bnl.gov/conferences/index.php/EIC_R&D`.

[32] "Electron-Ion Collider Detector Requirements and R&D Handbook (version 1.1)," Jan 2019. `http://eicug.org/web/sites/default/files/EIC_HANDBOOK_v1.1.pdf`.

[33] T. Polakovic, W. Armstrong, V. Yefremenko, J. Pearson, K. Hafidi, G. Karapetrov, Z.-E. Meziani, and V. Novosad, "Superconducting nanowires as high-rate photon detectors in strong magnetic fields," *Nucl. Instrum. Meth. A*, vol. 959, p. 163543, 2020.

[34] EIC Detector Advisory Committee, "Report of the 19th Electron Ion Collider Detector R&D Meeting," July 2020. `https://wiki.bnl.gov/conferences/images/5/53/EIC_Review_2020_July.pdf`.

[35] T. Polakovic, W. Armstrong, G. Karapetrov, Z.-E. Meziani, and V. Novosad, "Unconventional applications of superconducting nanowire single photon detectors," *Nanomaterials*, vol. 10, p. 1198, Jun 2020.

[36] "Doe basic research needs study on high energy physics detector research and development, report of the office of science workshop on basic research needs for hep detector research and development," 2019 (December 11-14, 2019). https://science.osti.gov/-/media/hep/pdf/Reports/2020/DOE_Basic_Research_Needs_Study_on_High_Energy_Physics.pdf.

[37] "High precision timing distribution project." https://espace.cern.ch/HighPrecisionTiming.

[38] C. E. P. Department, "Strategic r&d programme on technologies for future experiments," 2018. https://ep-dep.web.cern.ch/sites/ep-dep.web.cern.ch/files/Report%20final_0.pdf.

[39] "Cern GBT project." http://cern.ch/proj-gbt.

[40] "Cern dcdc project." http://project-dcdc.web.cern.ch.

[41] S. Bentvelsen, J. Engelen, and P. Kooijman, "Reconstruction of (x, Q**2) and extraction of structure functions in neutral current scattering at HERA," in *Workshop on Physics at HERA*, pp. 23–42, 1 1992.

[42] C. Adloff *et al.*, "Inclusive measurement of diffractive deep inelastic ep scattering," *Z. Phys.*, vol. C76, pp. 613–629, 1997.